QGP physics in fixed target collisions

Barbara Trzeciak
Czech Technical University in Prague

June 22-24, 2022
CERN

GAČR CZECH SCIENCE FOUNDATION

CTU CZECH TECHNICAL UNIVERSITY IN PRAGUE

Outline

1. Fixed target mode at LHC
   - Physics case

2. Light flavour probes
   - Charged particle multiplicity and elliptic flow
   - Longitudinal flow decorrelation
   - Global Lambda polarization

3. Heavy flavour probes
   - Quarkonium suppression
   - Open HF nuclear modification factor and elliptic flow
   - Open HF directed flow

Fixed target mode at LHC

➔ Energy range

7 TeV proton beam on a fixed target

c.m.s. energy: $\sqrt{s} = \sqrt{2m_N E_p} \approx 115\,\text{GeV}$	**Rapidity shift:**
Boost: $\gamma = \sqrt{s}/(2m_N) \approx 60$	$y_{c.m.s.} = 0 \rightarrow y_{lab} = 4.8$

2.76 TeV Pb beam on a fixed target

c.m.s. energy: $\sqrt{s_{NN}} = \sqrt{2m_N E_{\text{Pb}}} \approx 72\,\text{GeV}$	**Rapidity shift:**
Boost: $\gamma \approx 40$	$y_{c.m.s.} = 0 \rightarrow y_{lab} = 4.3$

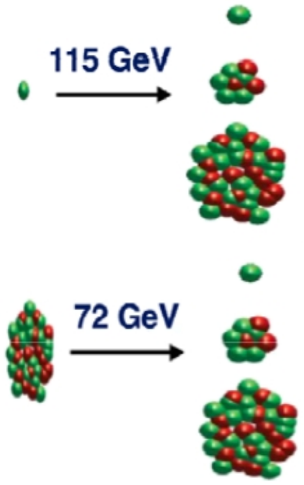

- √s in-between SPS and top RHIC

➔ Effect of boost

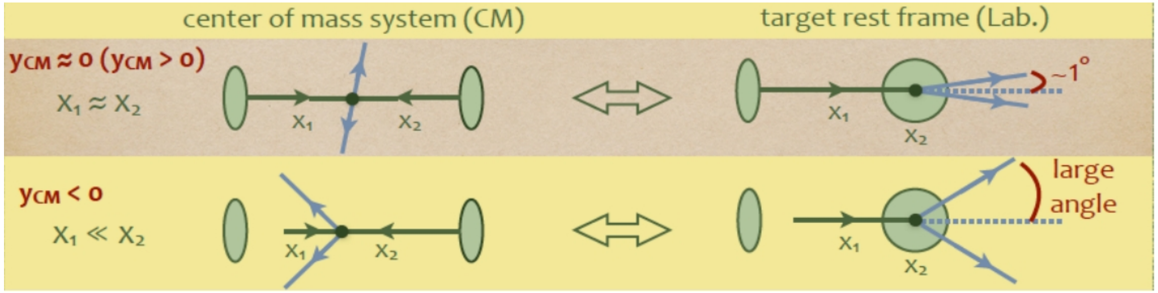

- Entire forward hemisphere, $y_{cms} > 0$, within 1 degree
- **Easy access to (very) large backward rapidity range, $y_{cms} < 0$**
- **And large parton momentum fraction $x_2 \rightarrow 1$ ($x_F \rightarrow -1$)**

Fixed target mode at LHC

➔ Energy range

7 TeV proton beam on a fixed target

c.m.s. energy:	$\sqrt{s}=\sqrt{2m_N E_p}\approx 115\,\mathrm{GeV}$	**Rapidity shift:**
Boost:	$\gamma=\sqrt{s}/(2m_N)\approx 60$	$y_{c.m.s.}=0\rightarrow y_{lab}=4.8$

2.76 TeV Pb beam on a fixed target

c.m.s. energy:	$\sqrt{s_{NN}}=\sqrt{2m_N E_{Pb}}\approx 72\,\mathrm{GeV}$	**Rapidity shift:**
Boost:	$\gamma\approx 40$	$y_{c.m.s.}=0\rightarrow y_{lab}=4.3$

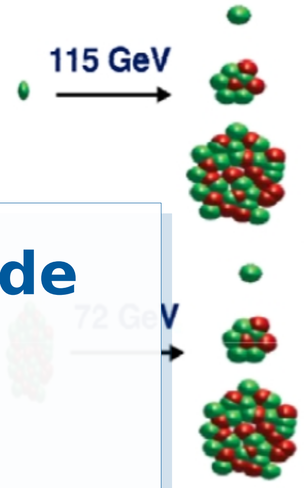

- √s in-between SPS and top RHIC

➔ Effect of boost

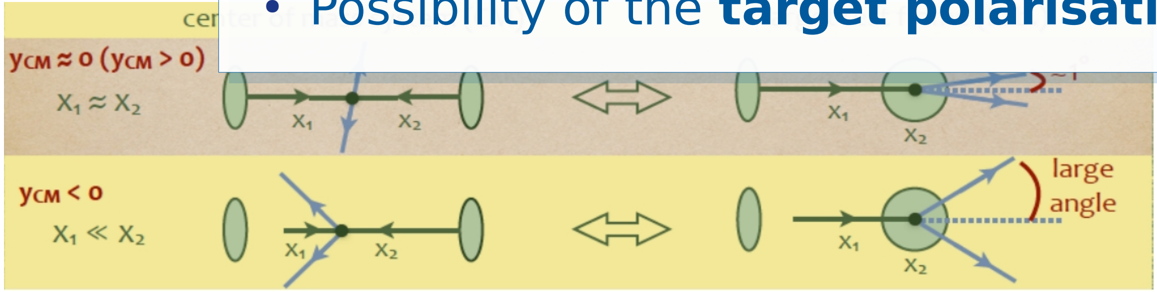

- Entire forward hemisphere, $y_{cms}>0$, within 1 degree
- **Easy access to (very) large backward rapidity range, $y_{cms}<0$**
- **And large parton momentum fraction $x_2\rightarrow 1$ ($x_F\rightarrow -1$)**

Advantages of a fixed-targed mode at the LHC

- Accessing **high-x frontier**
- Achieving **high luminosities**
- Varying **atomic mass number** of the target
- Possibility of the **target polarisation**

Physics motivations

- Advance our understanding of the **high-x frontier in nucleons and nuclei** (gluon and heavy-quark content) **and its connection to astroparticle physics**
- Unravel the **spin of the nucleon**: dynamics and spin distributions of quarks and gluons inside (un)polarised nucleons
- Studies of the **quark-gluon plasma** in heavy-ion collisions at a new energy domain down to the target-rapidity region

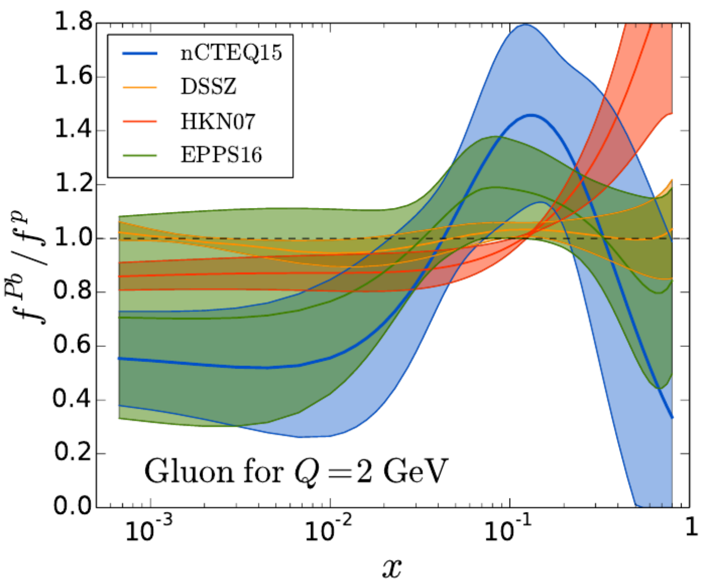

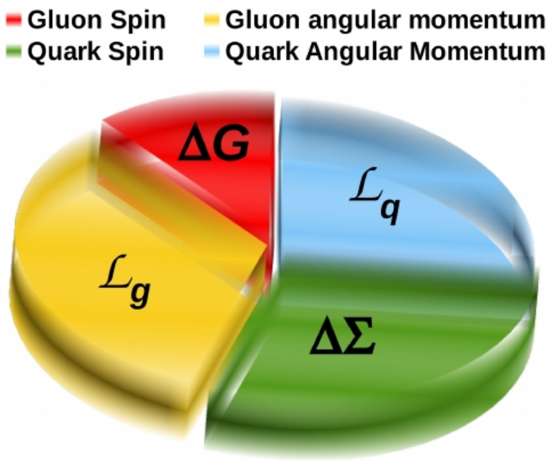

$$\frac{1}{2} = \frac{1}{2}\Delta\Sigma + \Delta G + \mathcal{L}_g + \mathcal{L}_q$$

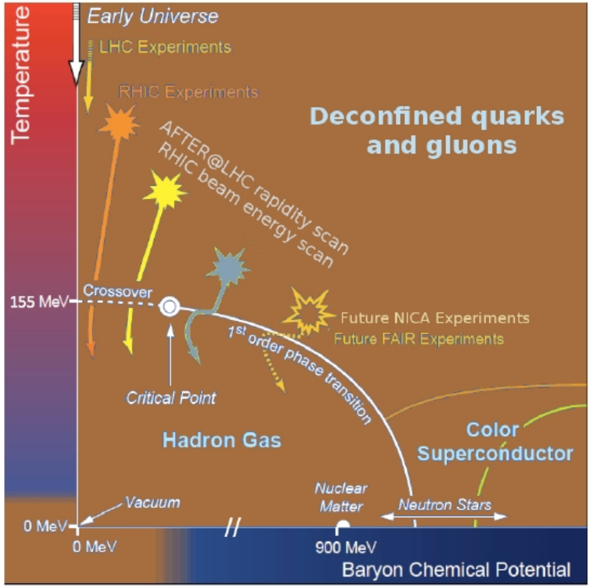

Physics case: QGP

- Study of the **quark-gluon plasma** between SPS and top RHIC energies of **$\sqrt{s_{NN}}$ = 72 GeV over broad rapidity range**
- Complete studies as a function of **rapidity, centrality and system size**
  - $\sqrt{s_{NN}}$ – between RHIC 54.4, 62.4 and 200 GeV
  - Scan in μ_B – complementary to RHIC BES programme
  - Scan in target-A and wide rapidity coverage – powerful constraints on models

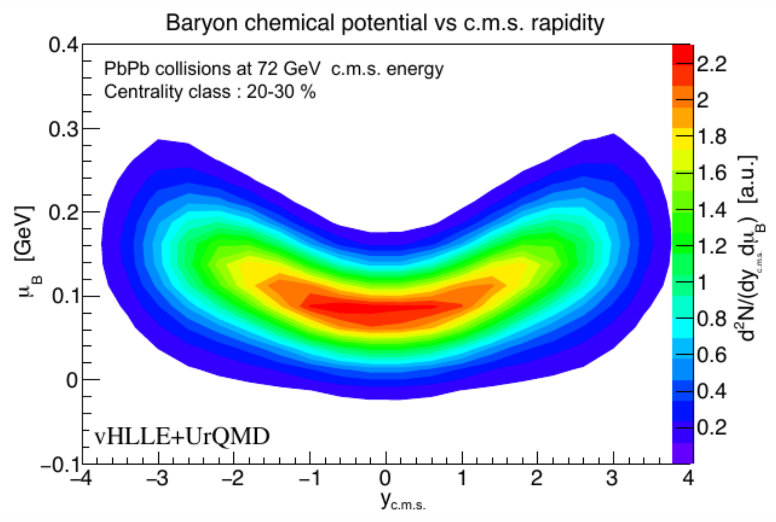

I.Karpenko, Acta Phys. Polon. B50 (2019), 141-148

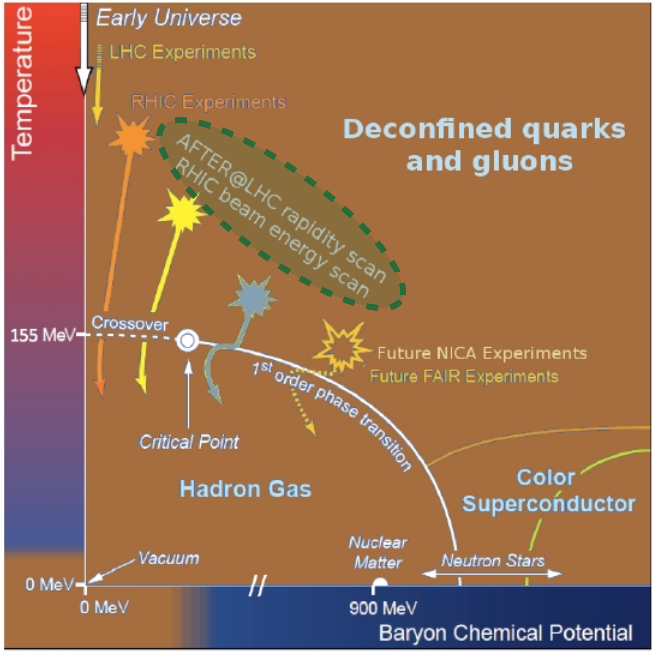

Bulk properties

- Initial state and longitudinal expansion of the medium
  - v_n vs y → temperature dependence of η/s
  - Longitudinal flow decorrelation → medium transport properties
  - Lambda polarization → medium vorticity

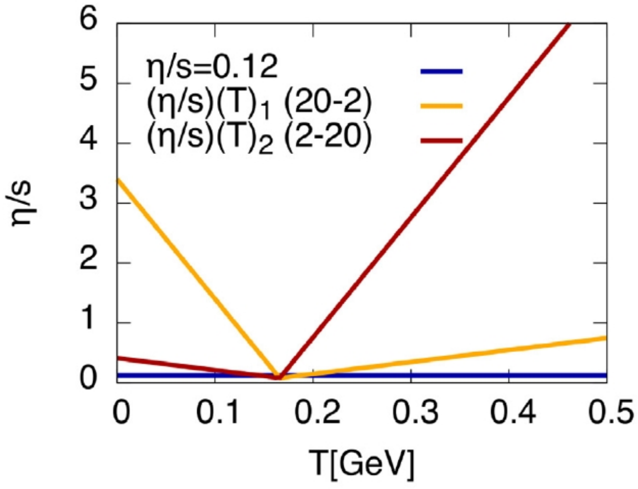

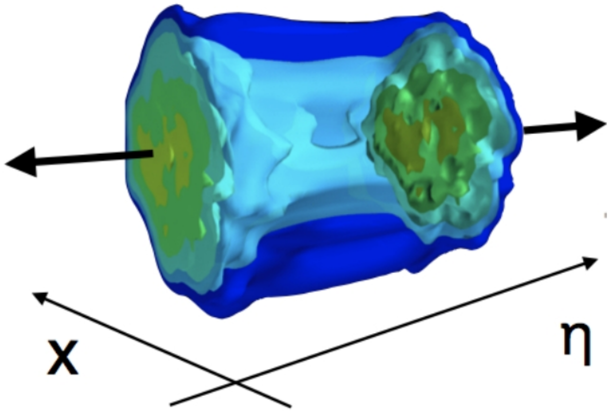

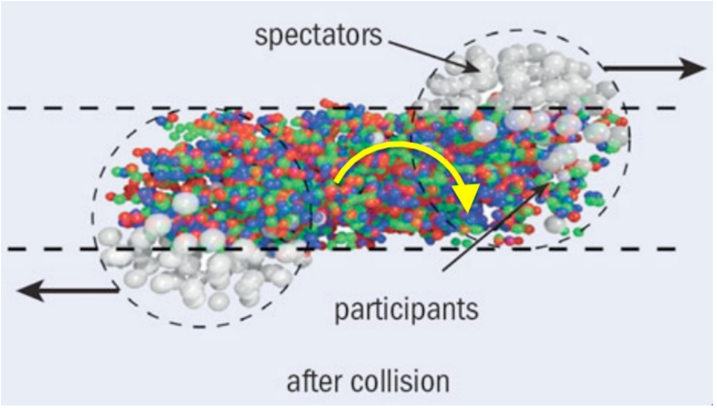

$dN_{ch}/d\eta$ and v_2 – initial state

- Event-by-event viscous hydrodynamic model
- Pb-W, Pb-Ti, Pb-C at 72 GeV with GLISSANDO and UrQMD initial states
  - Model tuned on basics observable from RHIC at 27 and 62 GeV and 200 GeV
    Phys. Rev. C 103, 034902 (2021)

$dN_{ch}/d\eta$ at 72 GeV

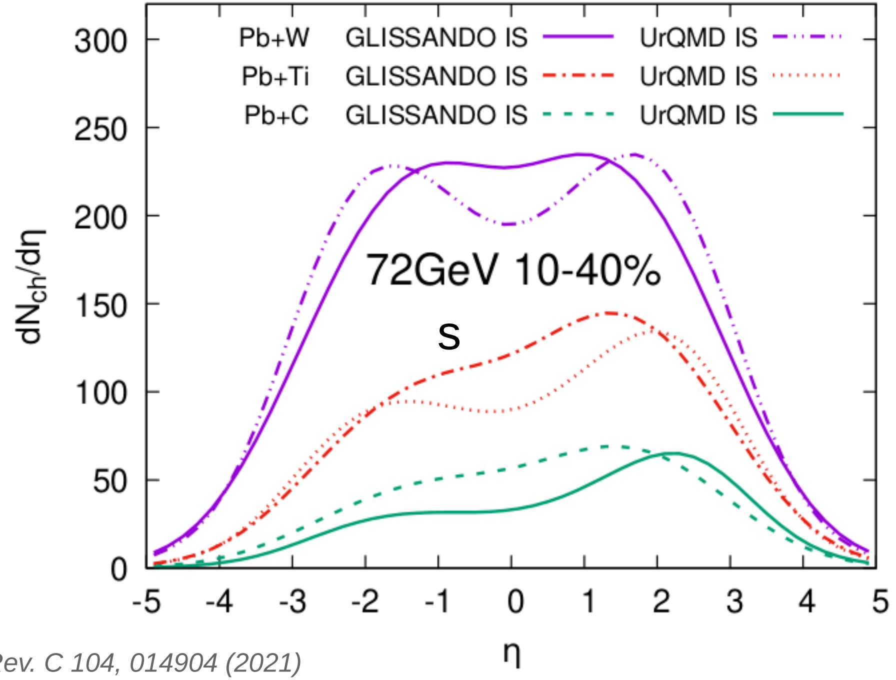

V_2 at 72 GeV

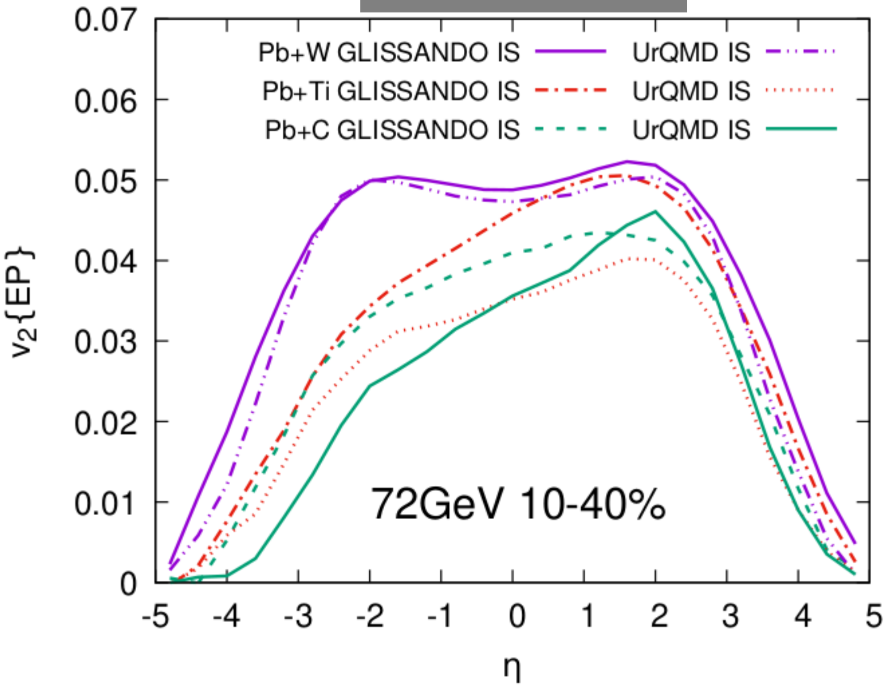

Phys. Rev. C 104, 014904 (2021)

v_2 – temperature dependence

- v_n vs y → temperature dependence of η/s
- High precision v_n studies will shed light on transverse and longitudinal dynamics in PbA and pA

$$\frac{d^2N}{dp_T d\phi} \propto \sum_{n=1}^{\infty} 2v_n(p_T)\cos(n(\phi - \Psi))$$

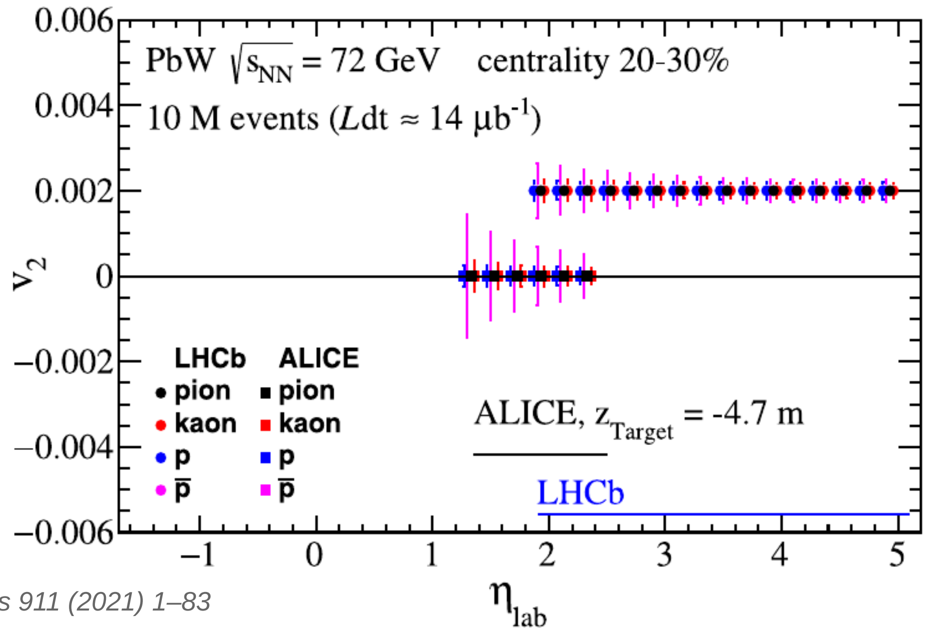

Physics Reports 911 (2021) 1–83

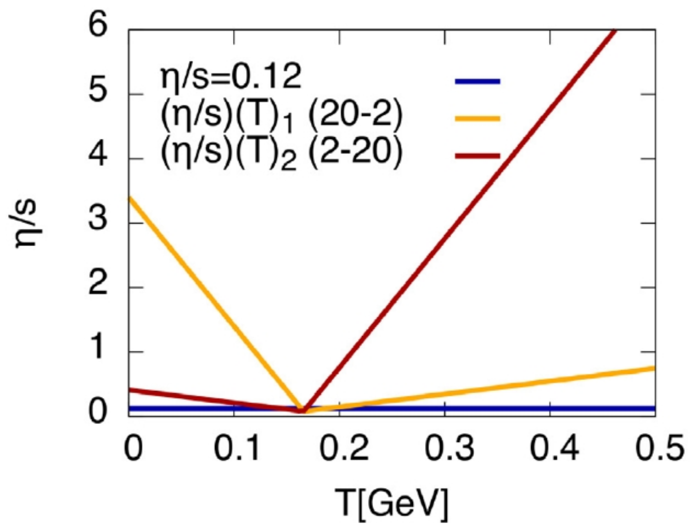

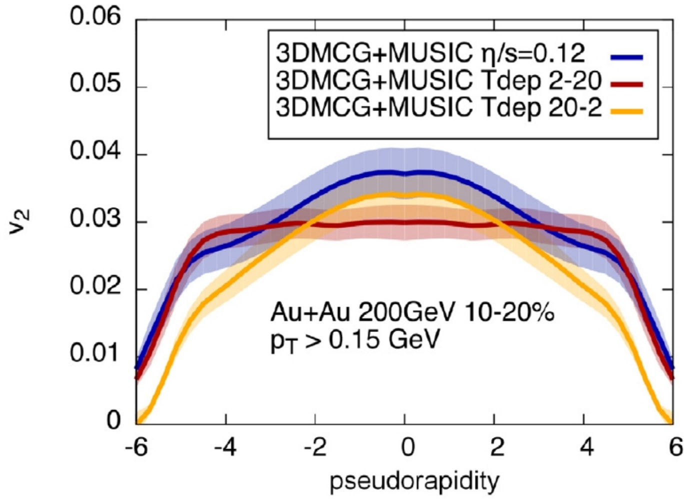

Longitudinal flow decorrelation

➔ Longitudinal dynamics of heavy-ion collisions

- Long. structure of flow → transport properties of QGP *Phys.Rev. C 98, 024913 (2018)*
- Sensitive to initial state

Requires:

- Modeling: full (3+1)D QGP evolution, source fluctuations
- Longitudinal fluctuations → EbE flow fluctuations in magnitude and direction

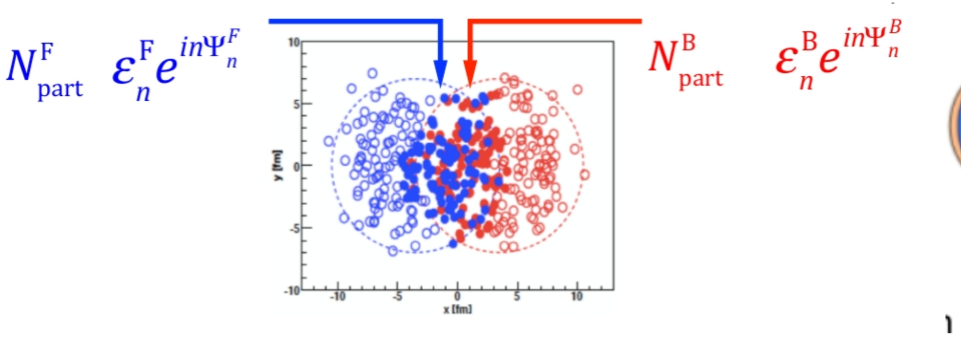

Forward & backward going participant distributions are not symmetric

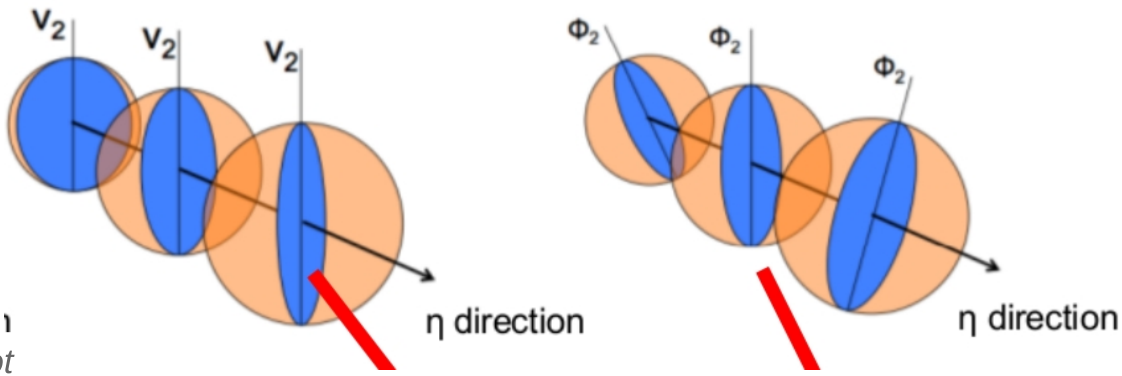

S.Mohapatra, QM17

Also, linear twist of the event-plane angle $\Psi_n(\eta)$ in the longitudinal direction was suggested in CGC model

Factorization ratio r_n

➔ **Factorization ratio r_n** – measure of the flow decorrelation

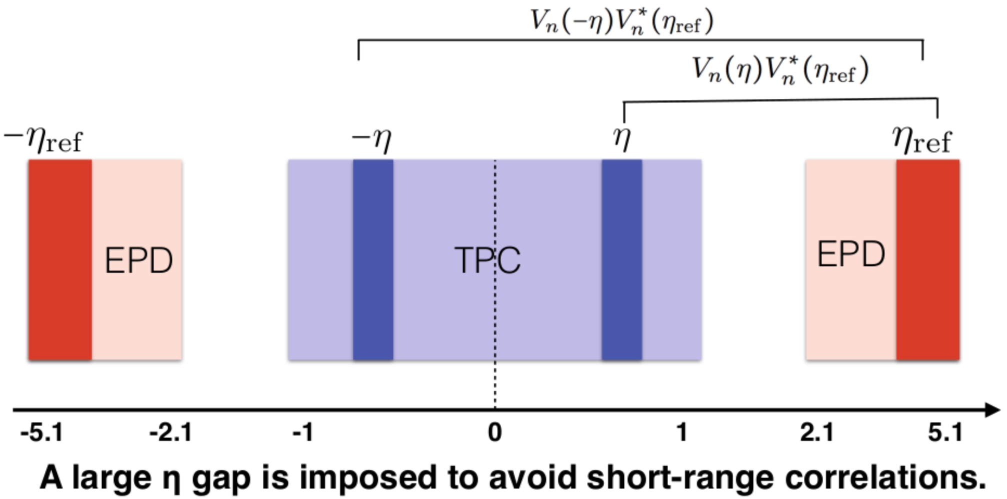

M.Nie, QM19

$$r_n(\eta) = \frac{\langle q_n(-\eta)q_n^*(\eta_{\rm ref})\rangle}{\langle q_n(\eta)q_n^*(\eta_{\rm ref})\rangle}$$

$$r_n(\eta) = \frac{\langle v_n(-\eta)v_n(\eta_{\rm ref})\cos[n(\Psi_n(-\eta)-\Psi_n(\eta_{\rm ref}))]\rangle}{\langle v_n(\eta)v_n(\eta_{\rm ref})\cos[n(\Psi_n(\eta)-\Psi_n(\eta_{\rm ref}))]\rangle}$$

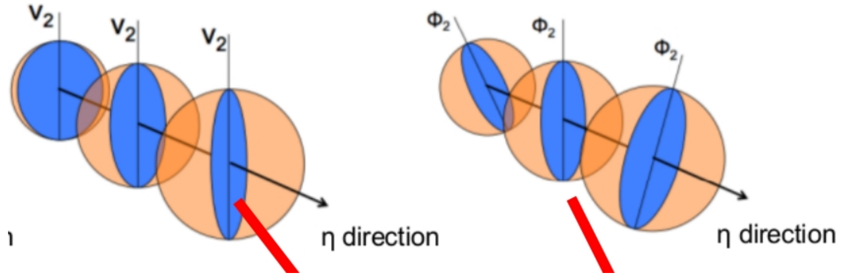

➔ Two effects:

- *flow magnitude decorrelation*
- *flow angle decorrelation*

Flow decorrelation

- **STAR**: r_2, r_3 measured at 200 and 27 GeV
  - Stronger decorrelation with decreasing energy

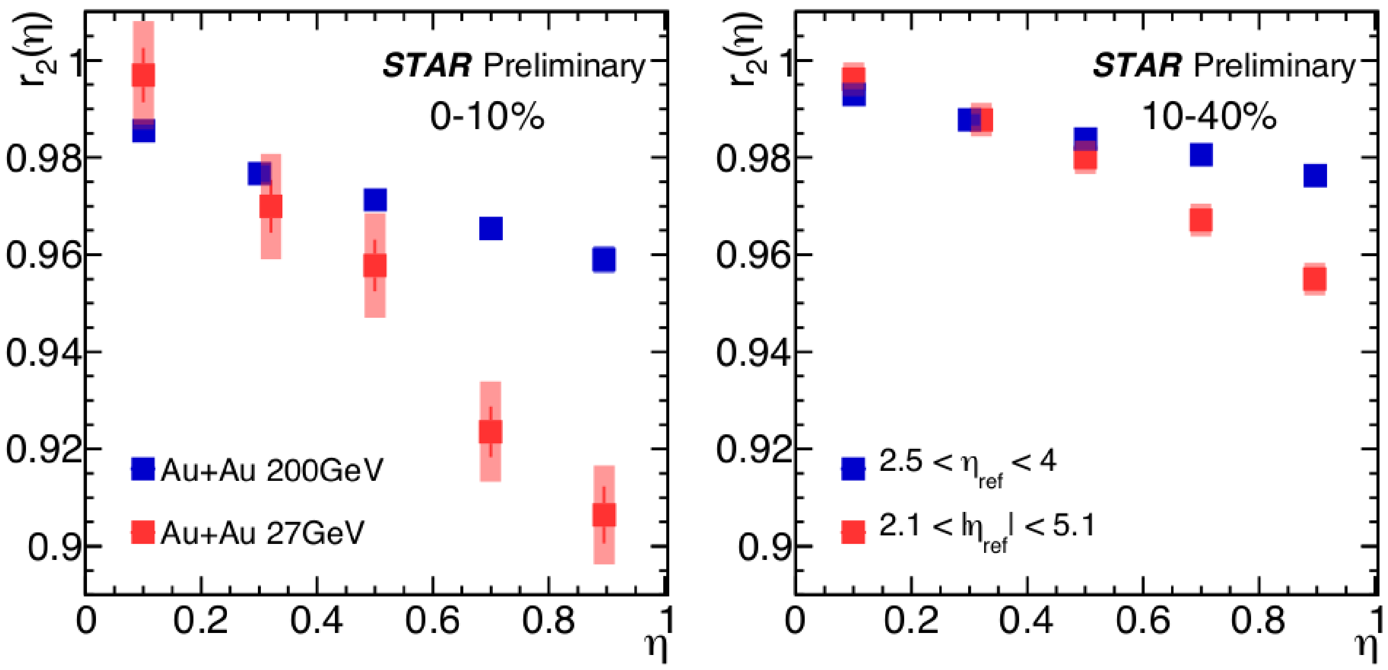

M.Nie, QM19
QM18

- **LHC:** CMS: Phys. Rev. C92 (3) (2015) 034911, ATLAS: Eur. Phys. J. C (2018) 78:142

Flow decorrelation vs η/y_{beam}

- **STAR**: r_2, r_3 measured at 200 and 27 GeV
  - Scaling of r_2 vs η/y_{beam} not understood. Choice of reference y w.r.t. beam y ?

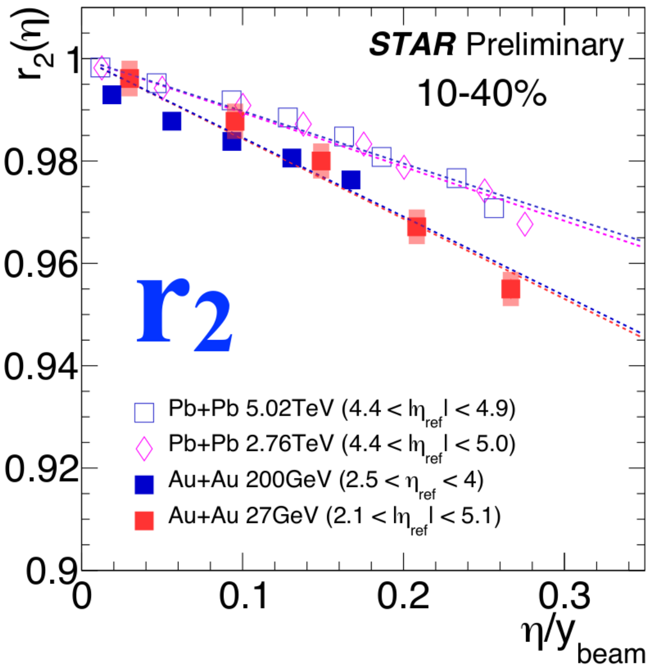

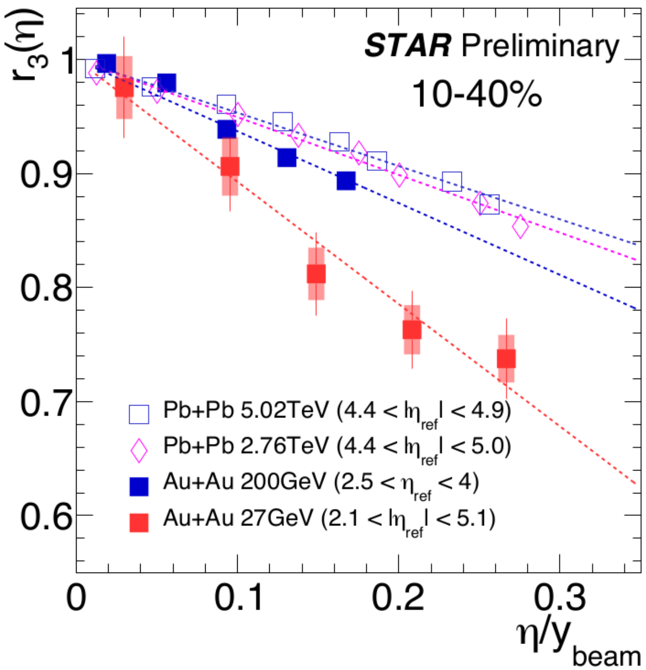

- Energy and system size studies of interest
- r_3 more sensitive to IS fluctuations

M.Nie, QM19

Decorrelation predictions – FTE@LHC

→ Event-by-event viscous hydrodynamic model: predictions for FTE@LHC

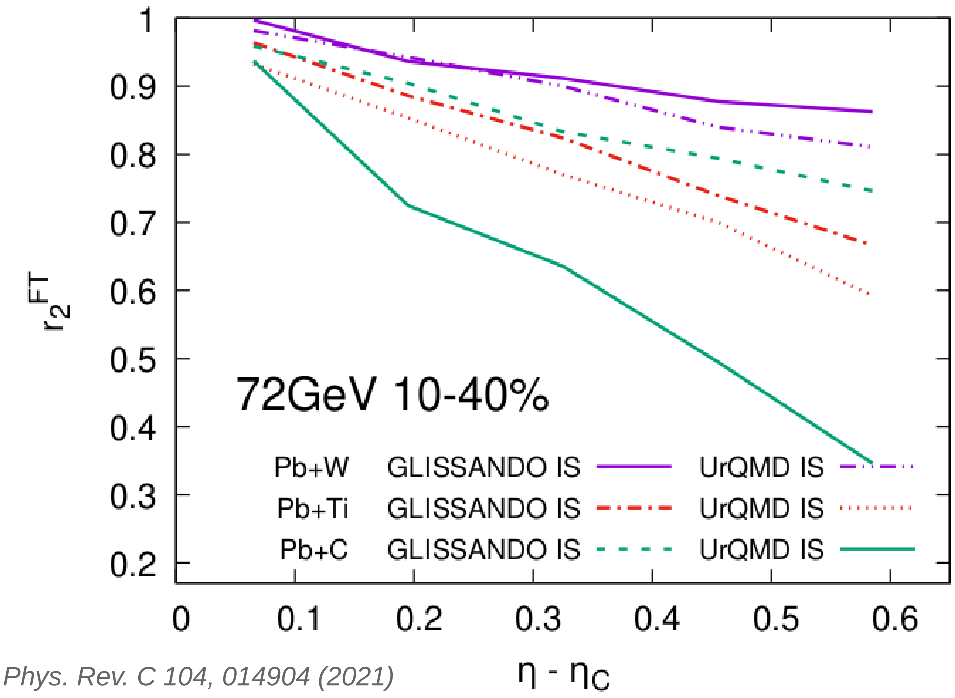

Phys. Rev. C 104, 014904 (2021)

→ **r_n definition**

- Fixed-target with two acceptance windows

$$r_n^{\mathrm{FT}}(\eta-\eta_C)=\frac{\langle q_n(-\eta+2\eta_C)q_n^*(\eta_{\mathrm{ref}})\rangle}{\langle q_n(\eta)q_n^*(\eta_{\mathrm{ref}})\rangle}$$

- *TPC:* $-2.9 < \eta < -1.6$
- *Muon det:* $-1.0 < \eta_{\mathrm{ref}} < -0.5$
- *Decorrelation around the center of the pseudo-rapidity bin:* $\eta_C = -2.25$

→ Strong decorrelation, increasing with decreasing system size

→ Significant differences between different IS models

Global Lambda polarization

- Non-central collisions: large orbital angular momentum
- Hadron spin alignment, P_H, with J via parton scattering: QCD spin-orbit coupling
- Hydro: thermal vorticity in fluid cells considered.
  Local thermodynamic equilibrium: vorticity transferred to hadron spin

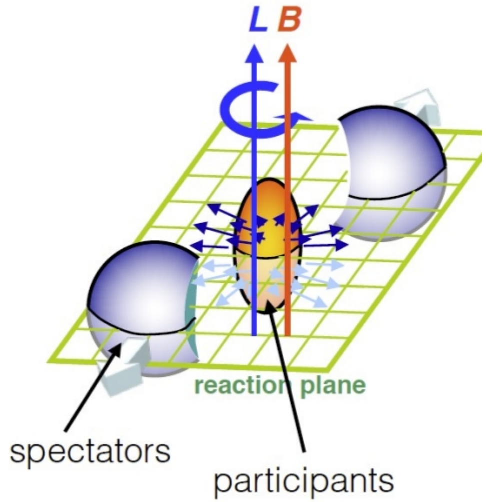

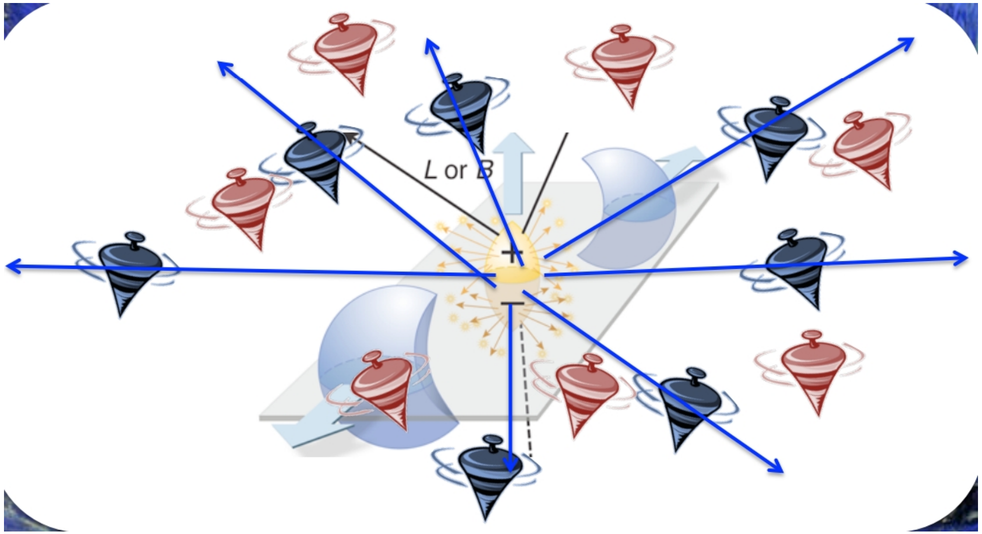

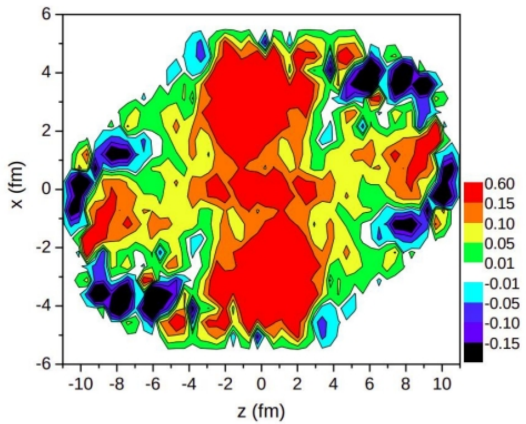

Becattini F, Csernai L, Wang DJ. Phys. Rev. C88034905(2013), Erratum: Phys. Rev.C 93 6 069901(2016)

Global Lambda polarization (2)

- Non-central collisions: large orbital angular momentum
- Hadron spin alignment, P_H, with J via parton scattering: QCD spin-orbit coupling
- Hydro: thermal vorticity in fluid cells considered.
  Local thermodynamic equilibrium: vorticity transferred to hadron spin

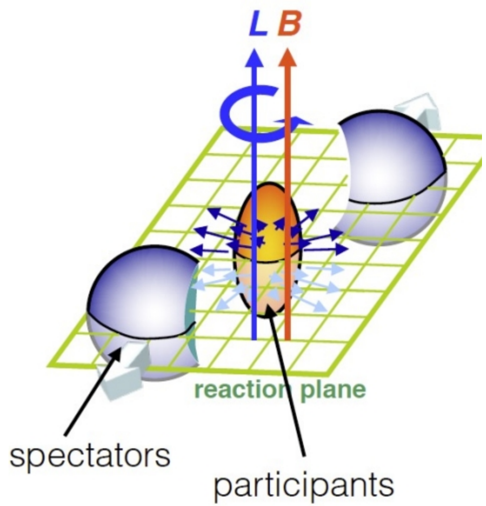

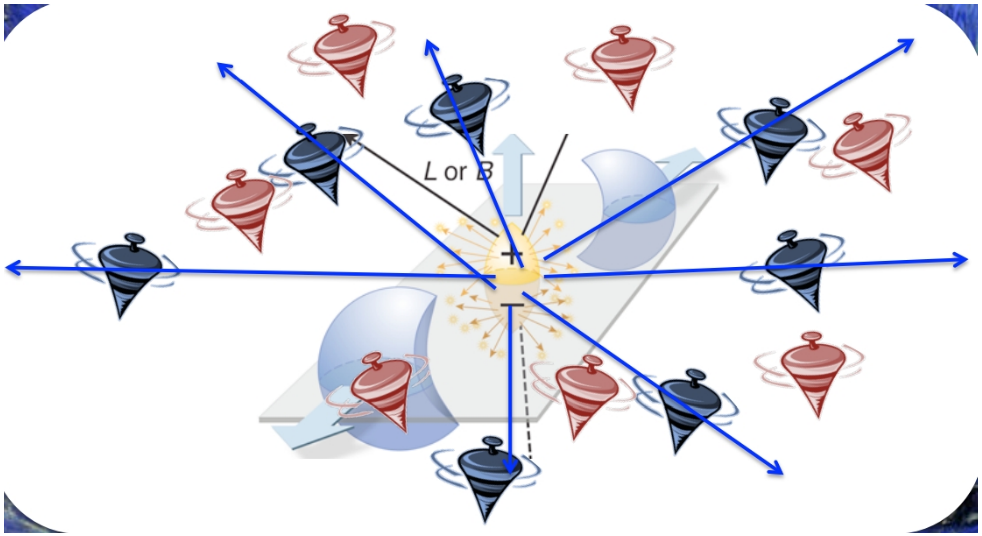

Fluid vorticity → Λ, anti-Λ in same direction

$$\omega = k_B T (P_\Lambda + P_{\bar{\Lambda}})/\hbar$$

Magnetic field → Λ, anti-Λ in opposite direction

$$B = \frac{T}{2\mu_\Lambda}(P_\Lambda - P_{\bar{\Lambda}})$$

$\vec{P}_{\bar{\Lambda}} \,||\, \vec{B}$ $\quad$ $\vec{P}_{\Lambda} \,||\, -\vec{B}$

$$\vec{\mu}_{B,\Lambda} = -\vec{\mu}_{B,\bar{\Lambda}}$$

Measurement of Lambda polarization

- Non-central collisions: large orbital angular momentum → vorticity
- Late-stage magnetic field sustained by the QGP → Λ, anti-Λ splitting (?)

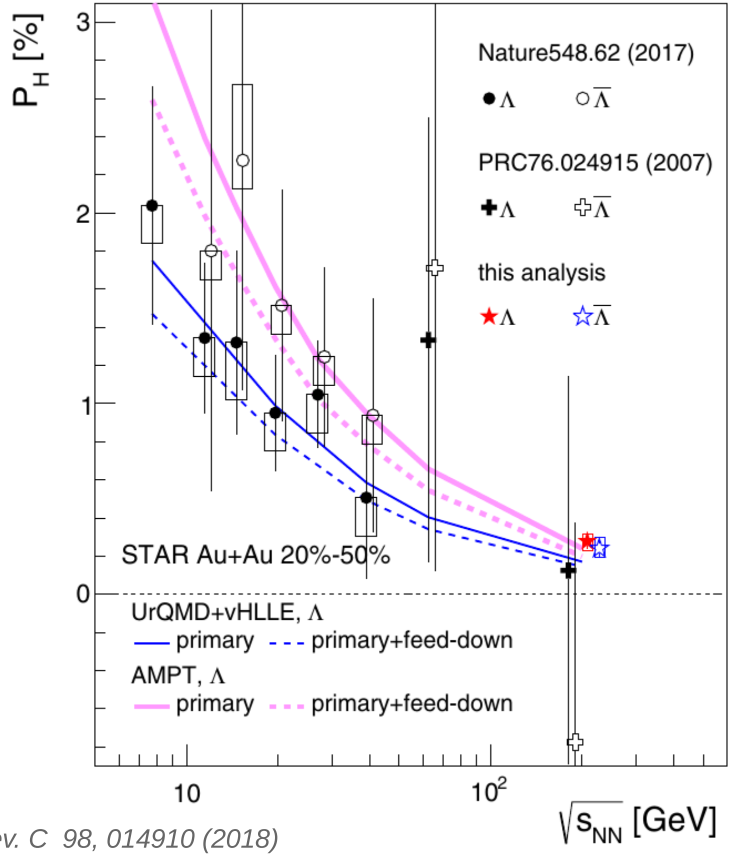

Phys. Rev. C 98, 014910 (2018)

- Parity-violating decay of hyperon
- Daughter proton preferentially decays along the Λ's spin (opposite for anti-Λ)
- Polarization measured via the distribution of the azimuthal angle of the daughter proton in the hyperon rest frame

$$P_H = \frac{8}{\pi \alpha_H} \frac{\langle \sin(\Psi_1 - \phi_d^*) \rangle}{\mathrm{Res}(\Psi_1)}$$

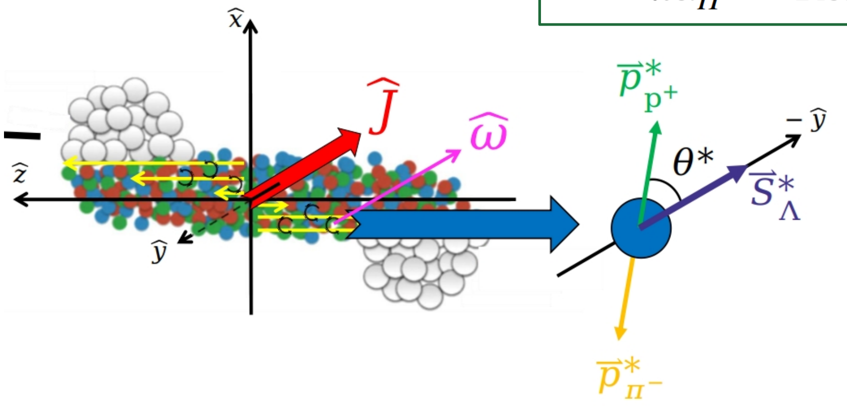

Global Lambda polarization at FTE@LHC

- Rapidity dependence → powerful constraints on models
- (Local lambda polarization, P_Z → additional constrains on shear viscosity)

Y. Jiang, *et al.*, Phys. Rev. C 94, 044910 (2016)

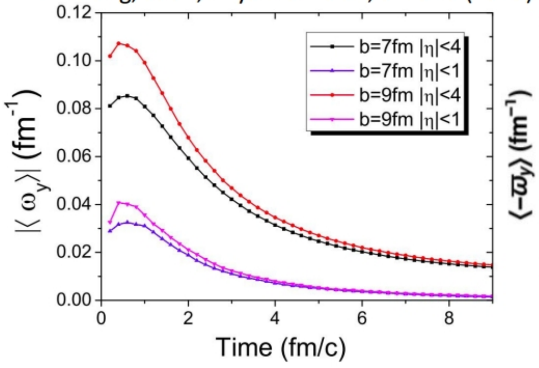

W.-T.Deng and X.-G Huang:PRC93,064907

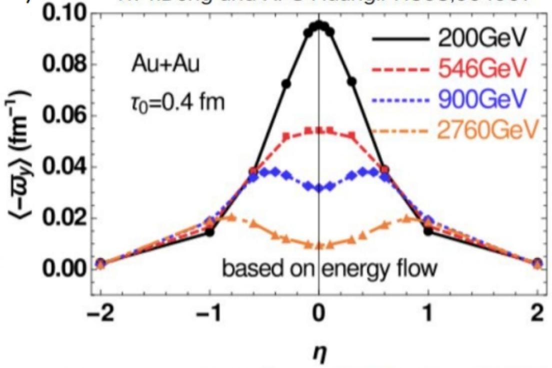

H.-Z. Wu, *et al.* , PR Research. 1, 033058 (2019)

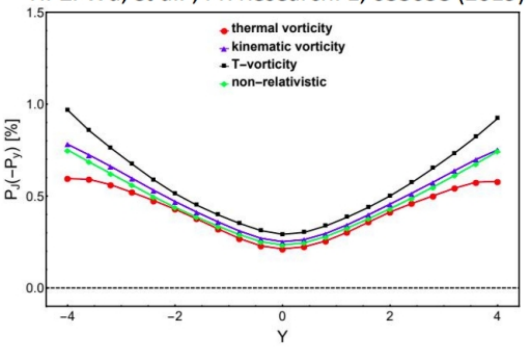

Z.T.Liang et al., Chin.Phys.C 45 (2021) 1, 014102

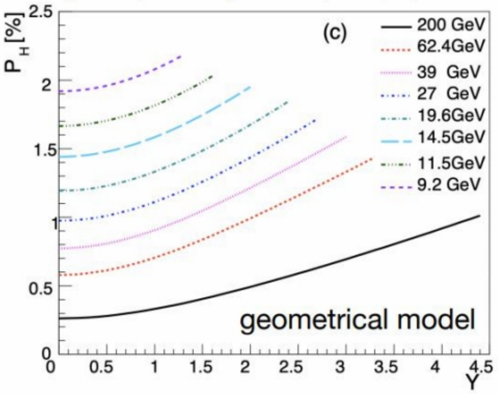

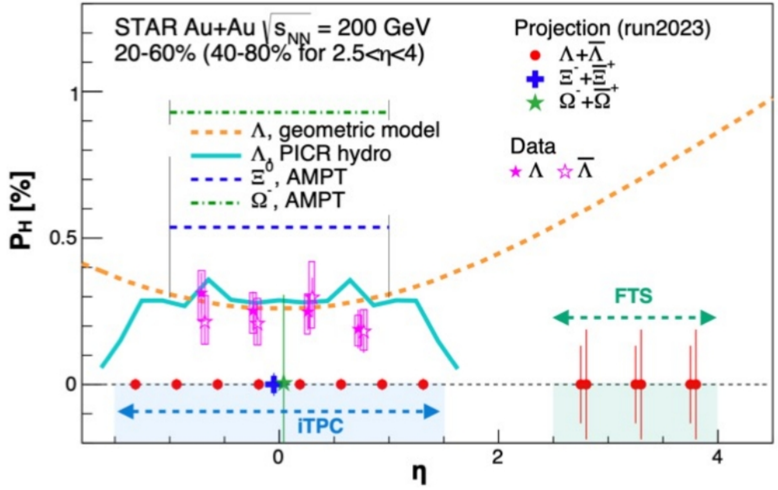

- Model predictions for FTE@LHC ongoing

Global Lambda polarization at FTE@LHC (2)

- System size dependence → P_H increases not only with decreasing energy but also with smaller system size
- With good statistics: Lambda, anti-Lambda splitting → magnetic field at freeze-out

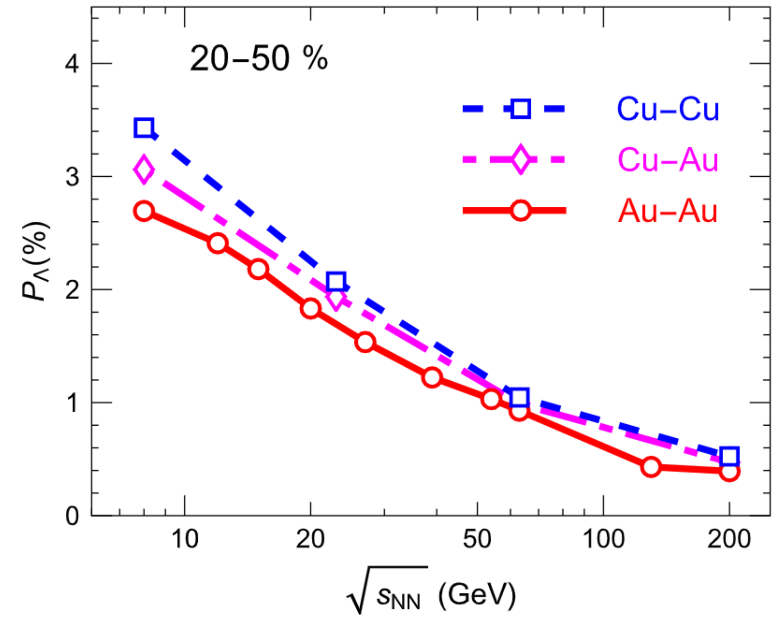

Phys. Lett. B788 (2019) 409-413

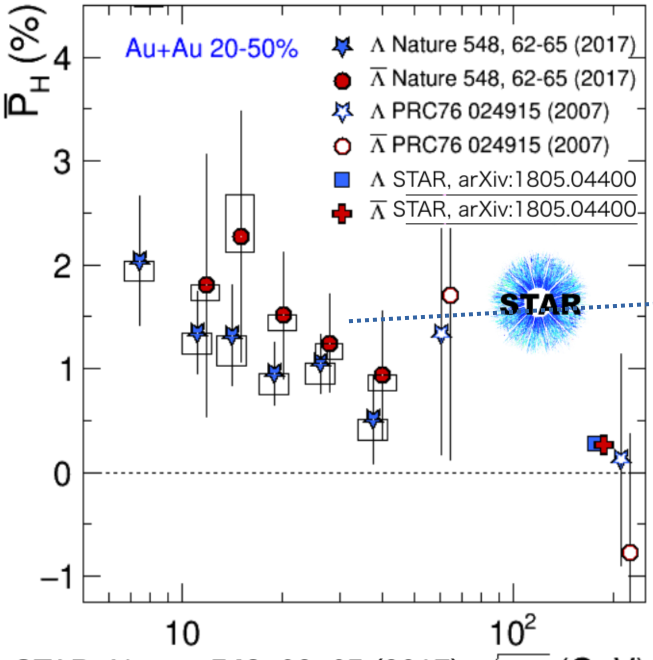

STAR, Nature **548**, 62–65 (2017) $\sqrt{s_{NN}}$ (GeV)

$$P_\Lambda \simeq \frac{1}{2}\frac{\omega}{T} + \frac{\mu_\Lambda B}{T}$$
$$P_{\bar{\Lambda}} \simeq \frac{1}{2}\frac{\omega}{T} - \frac{\mu_\Lambda B}{T}$$

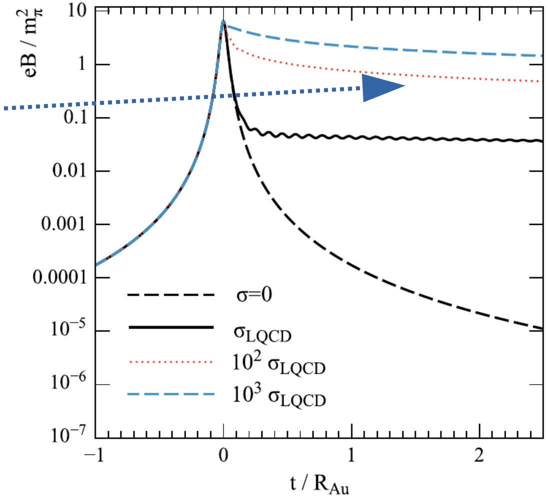

Nuclear Physics A 929 (2014) 184–190

Heavy flavour probes

➔ Unique access to heavy-flavour probes at this energy domain

- Quarkonium suppression in QGP → thermodynamic properties of QGP
- Open heavy-flavour → heavy-flavour energy loss, transport parameters of the QGP, hadronization
- Directed flow v_1 → initial tilt of the produced matter, QGP conductivity

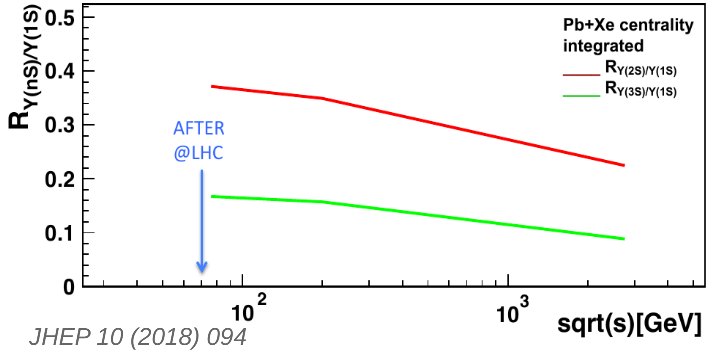

JHEP 10 (2018) 094

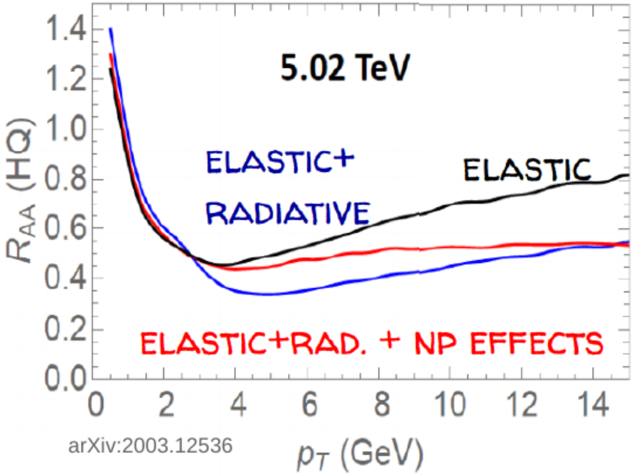

arXiv:2003.12536

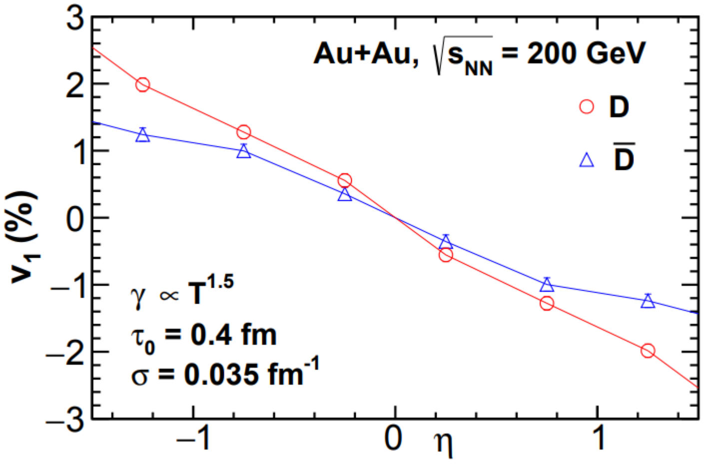

Phys. Lett. B798 (2019) 134955

Quarkonium studies

- Suppression of quarkonia in the medium – colour screening effect, recombination
- Effects beyond the static screening, feed down, cold nuclear matter effects
  - Quarkonium sequential suppression as the medium thermometer ? Bottomonia may provide clearer picture
  - Charmonia – significantly larger cross sections

Mid-rapidity J/ψ

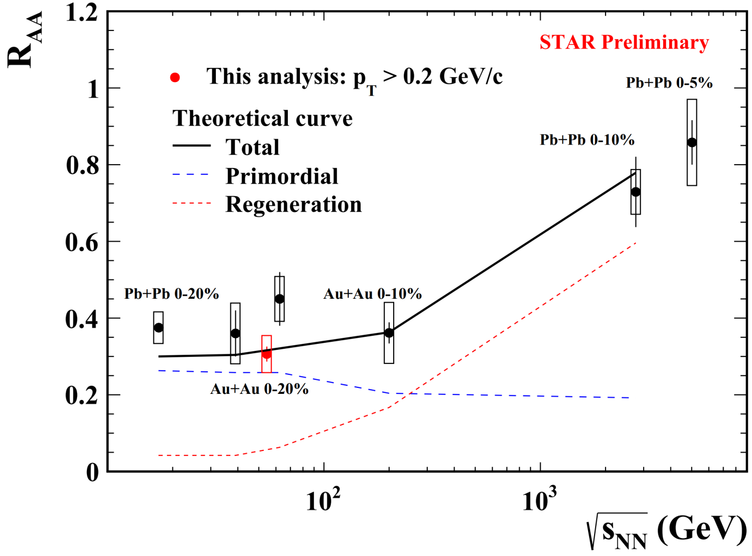

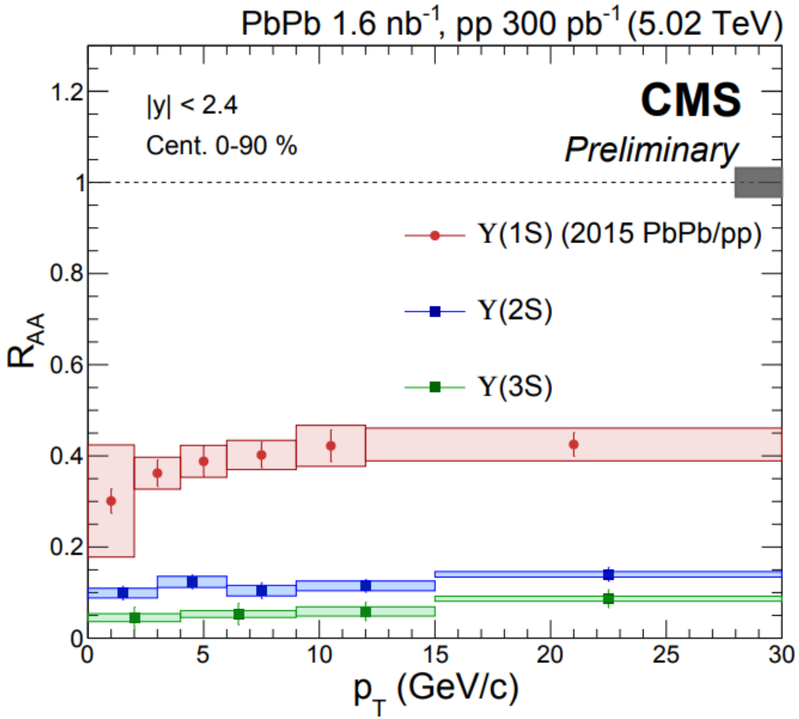

CMS PAS HIN-21-007

Quarkonium studies at FTE@LHC

- Quarkonia suppression in the medium – colour screening effect, recombination
  - Measurements of quarkonium states down to 0 p_T in pp, p-A and Pb-A
  - Negligible contribution from recombination
  - Possibility to measure Upsilon(nS) state suppression

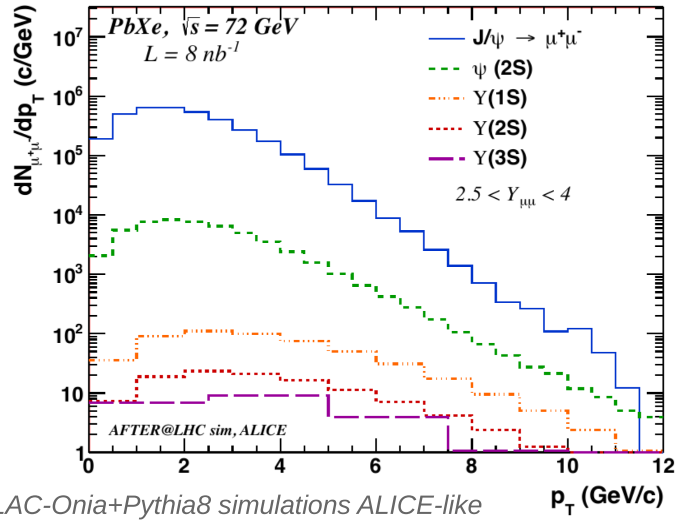

HELAC-Onia+Pythia8 simulations ALICE-like

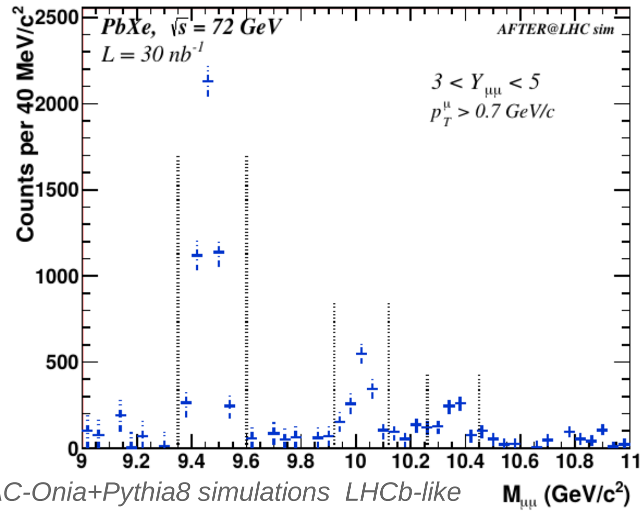

HELAC-Onia+Pythia8 simulations LHCb-like

Few Body Syst. 58 (2017) 5, 148

- With high charmonium rates – interesting to access χ_C and η_C, J/ψ – J/ψ and J/ψ – D correlations

Open HF measurements – D_s

- Simultaneous measurements of D meson elliptic flow and nuclear modification factor, in different systems
  - charm diffusion coefficient (D_s) and its temperature dependence
  - energy loss mechanism (collisional vs radiative)

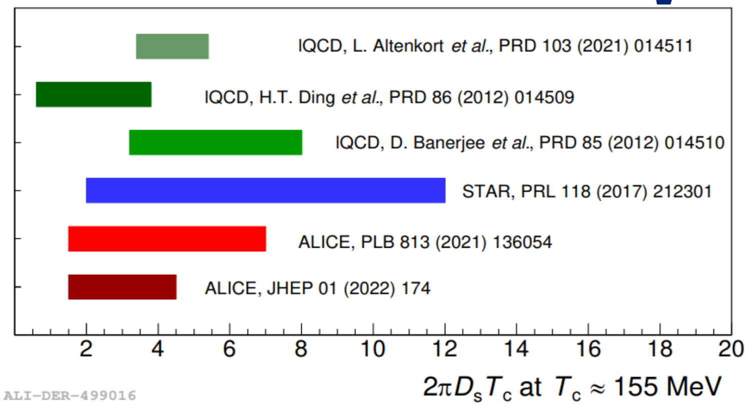

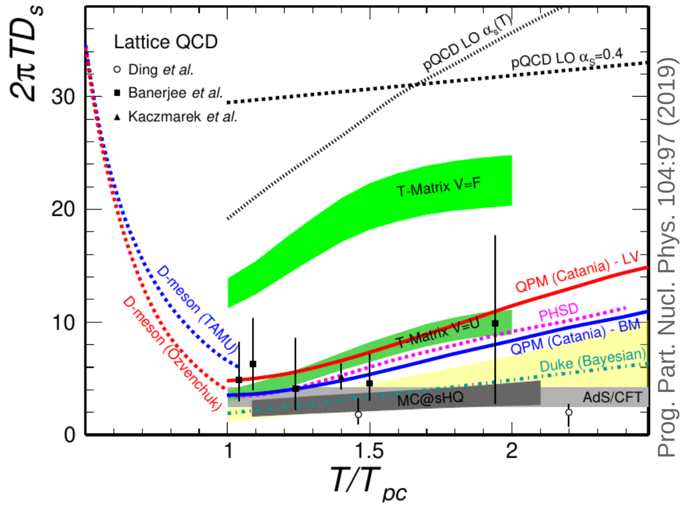

HF v_2 at 54.4 GeV

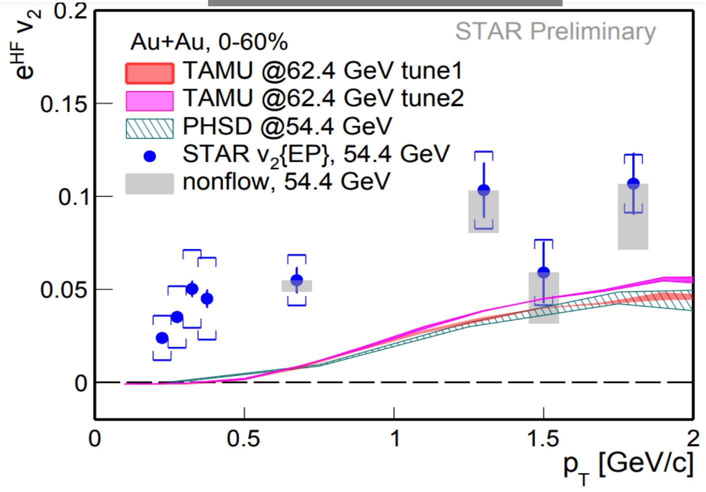

Open HF measurements

- Simultaneous measurements of D meson elliptic flow and nuclear modification factor, in different systems
  - charm diffusion coefficient (D_s) and its temperature dependence
  - energy loss mechanism (collisional vs radiative)

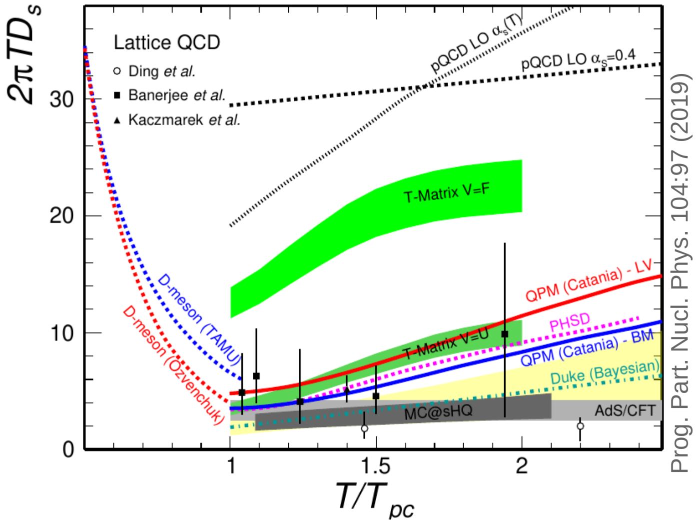

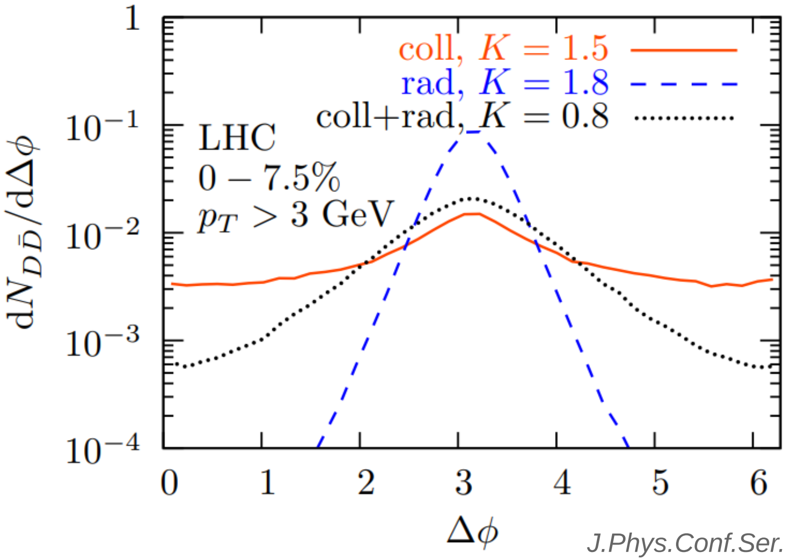

J.Phys.Conf.Ser. 509 (2014) 012047

- Correlation studies → potentially more constrains for energy loss models
- HF μ can be studied with ALICE muon arms at: -1.6 < y_{CMS} < -0.5

Open HF in small systems

- p-A collisions: cold nuclear matter effects, collectivity in small systems, QGP ?
- Simultaneous measurements of D meson R_{pA} and v_2 in different systems

0-10% centrality

R_{CP}

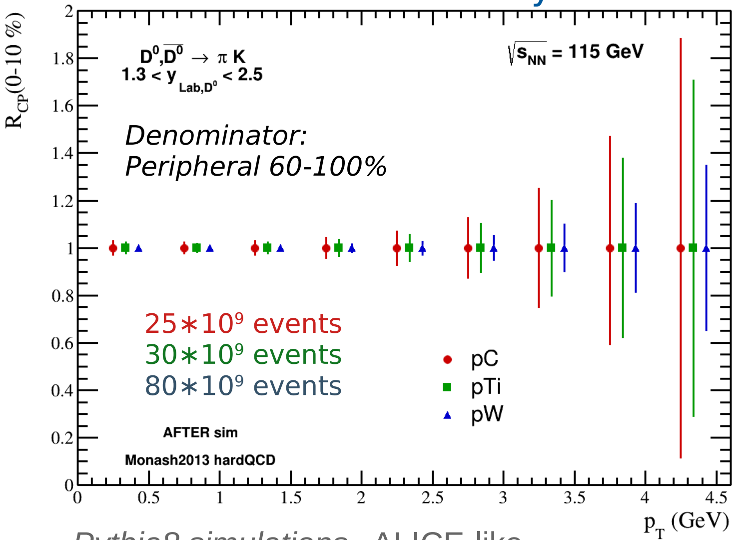

Pythia8 simulations ALICE-like

0-10% centrality

v_2

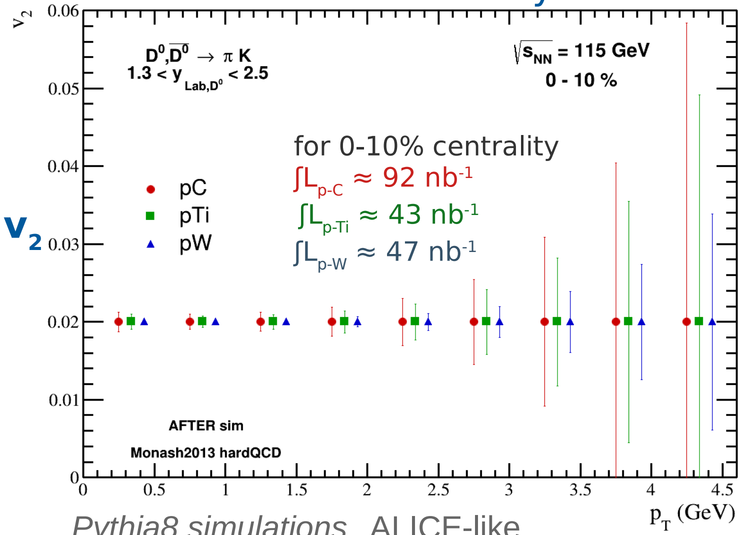

Pythia8 simulations ALICE-like

- HF μ can be studied with ALICE muon arms at: $-1.6 < y_{CMS} < -0.5$

HF directed flow, v_1

- Insights into initial tilt of matter and strong EM field in non-central HI collisions

Tilt

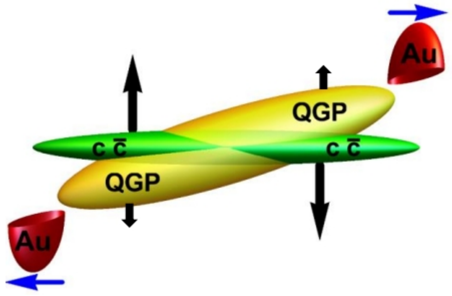

EM field

Charged-dependent v_1,
Sensitive to QGP conductivity

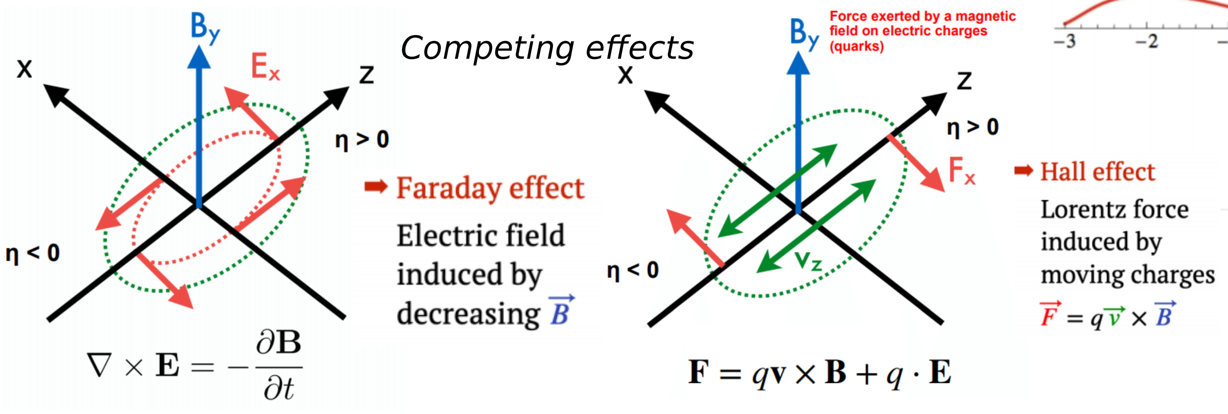

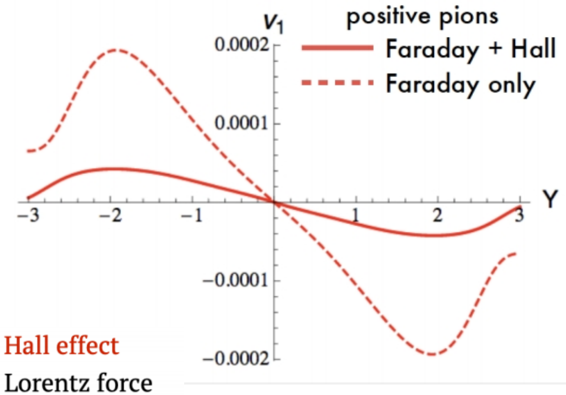

$$v_1 = \langle cos(\phi_p) \rangle = \langle p_x / p_T \rangle$$

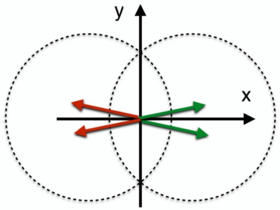

- v_1: sensitivity to the three-dimensional spatial profile of initial conditions and pre-equilibrium early time dynamics in the evolution

HF directed flow, v_1

- Insights into initial tilt of matter and strong EM field in non-central HI collisions
- Heavy-quarks:
  - produced early, shifted from the bulk
  - formation time comparable to when B is maximum

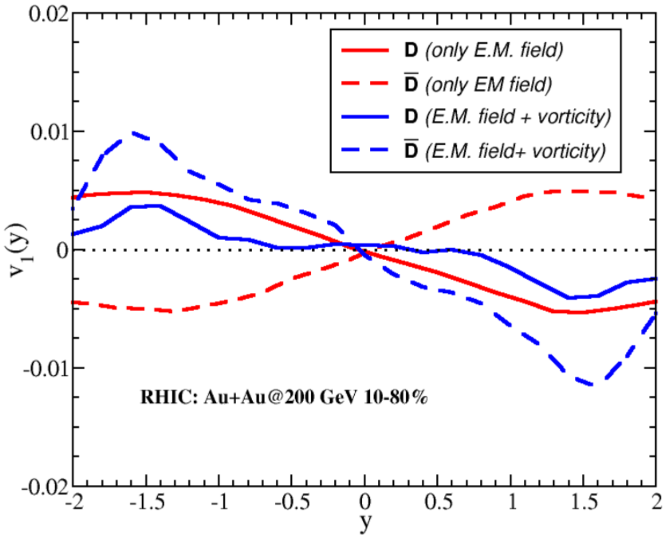

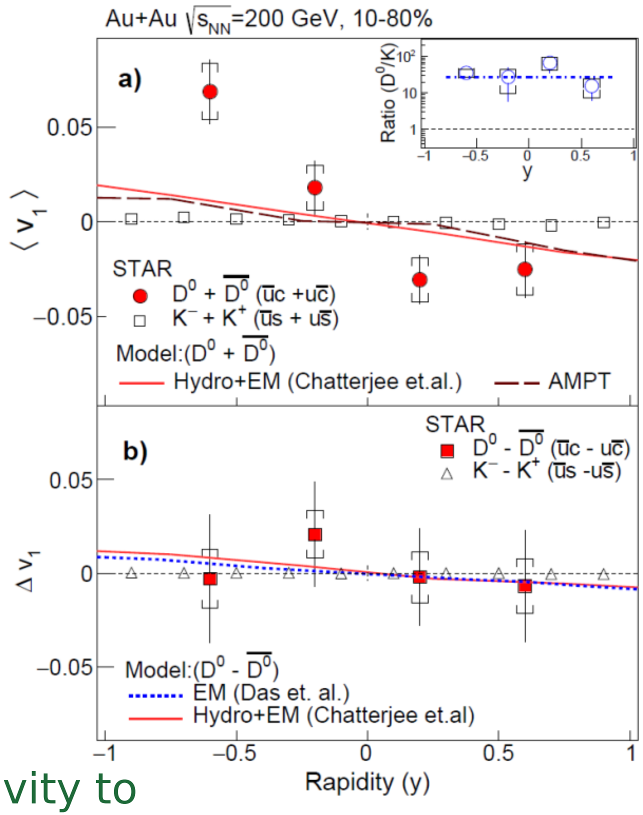

- Effect much larger than for light hadrons → strong sensitivity to the initial tilt and QGP transport parameters
- v_1 increases with rapidity; EM field: splitting between D^0 and $\overline{D^0}$

Summary

- AFTER@LHC: **high-statistics measurements in an energy domain between the SPS and top RHIC**, in an unexplored rapidity domain

- Study of the **quark-gluon plasma at $\sqrt{s_{NN}}$ = 72 GeV over broad rapidity range**

- Complete studies as a function of **rapidity, centrality and system size**
  - $\sqrt{s_{NN}}$ – between RHIC 54.4, 62.4 and 200 GeV
  - Scan in μ_B – complementary to RHIC BES programme
  - Scan in target-A and wide rapidity coverage – powerful constraints on models

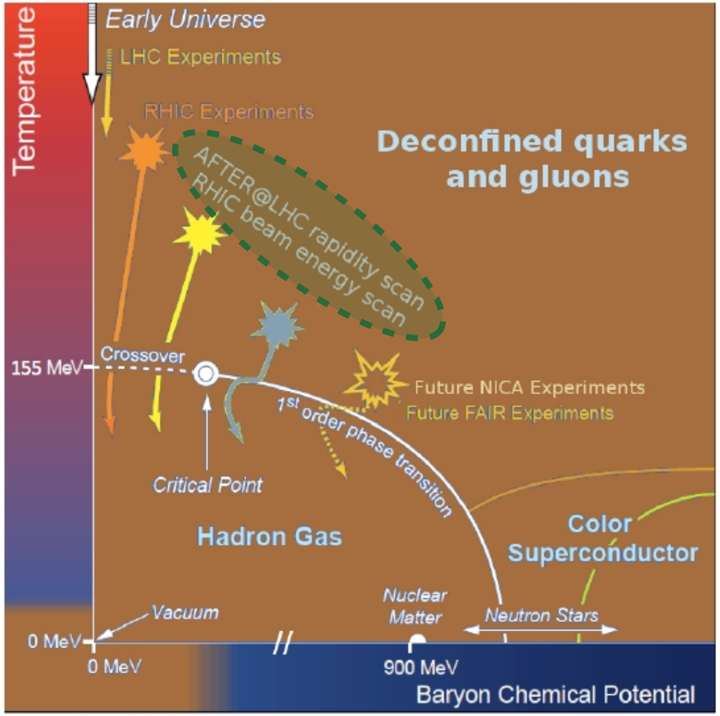

This work was supported by grant from The Czech Science Foundation, grant number: GJ20-16256Y

Backup

Anisotropic Flow in HI

- Collision geometry: initial spacial anisotropy
- Multiple interactions between (thermalized) constituents of the medium → azimuthal momentum space anisotropy of particle emission → flow
- Asymmetry between the **in-plane** and **out-of-plane** directions.

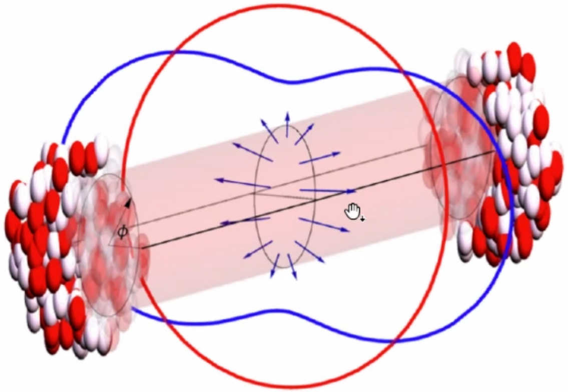

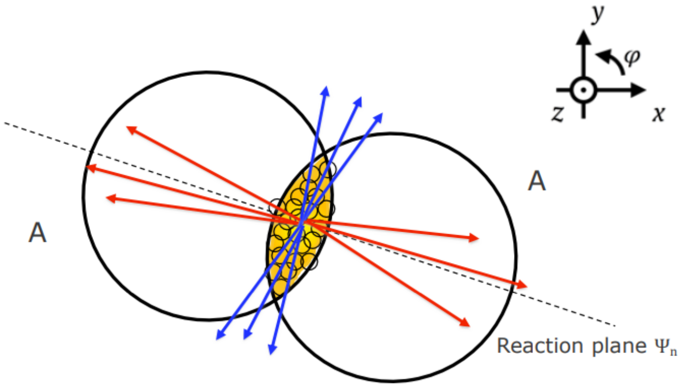

$$E\frac{d^3N}{dp_T} = \frac{1}{2\pi}\frac{d^2N}{p_T dp_T dy}\left\{1 + \sum_{n=1}^{\infty} v_n \cos[n(\varphi - \Psi_n)]\right\}$$

$$v_2 = \langle \cos[2(\varphi - \Psi_2)] \rangle$$

second harmonic coefficient
elliptic flow

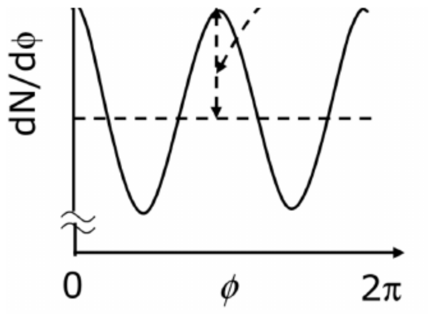

HF Elliptic Flow

- Heavy-flavour elliptic flow, v_2
  - Low p_T: Collective motion of the system; HQ thermalization ?
  - High p_T: Path-length dependent parton energy loss
- **Strong charm quark coupling with the medium at RHIC**

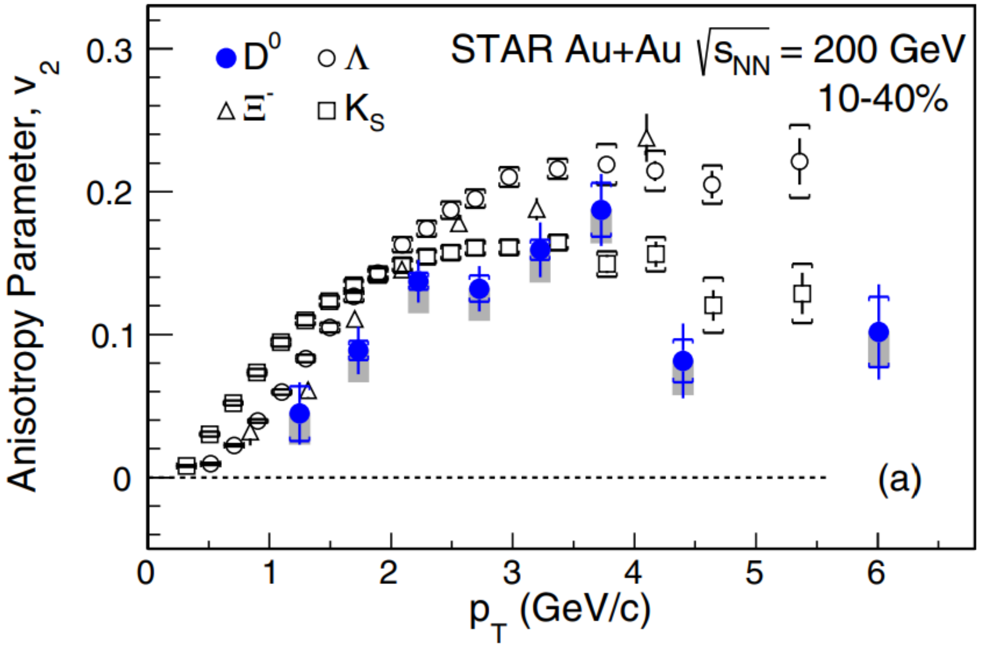

STAR: PRL 118, 212301 (2017)

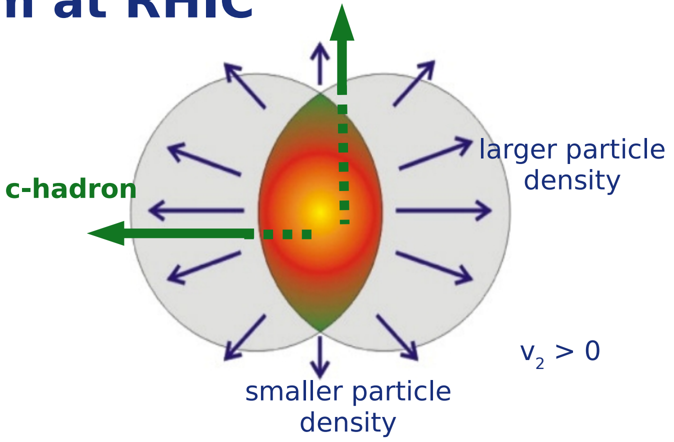

$$v_2 = \langle \cos[2(\varphi - \Psi_2)] \rangle$$

Open HF in small systems

- p-A collisions: cold nuclear matter effects, collectivity in small systems, QGP ?
- Simultaneous measurements of D meson elliptic flow and nuclear modification factor, in different systems

0-10% centrality

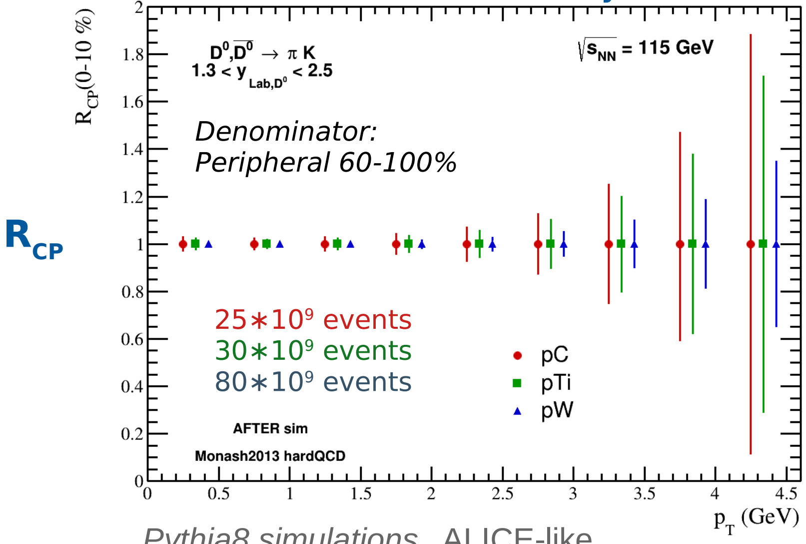

Pythia8 simulations ALICE-like

0-10% centrality

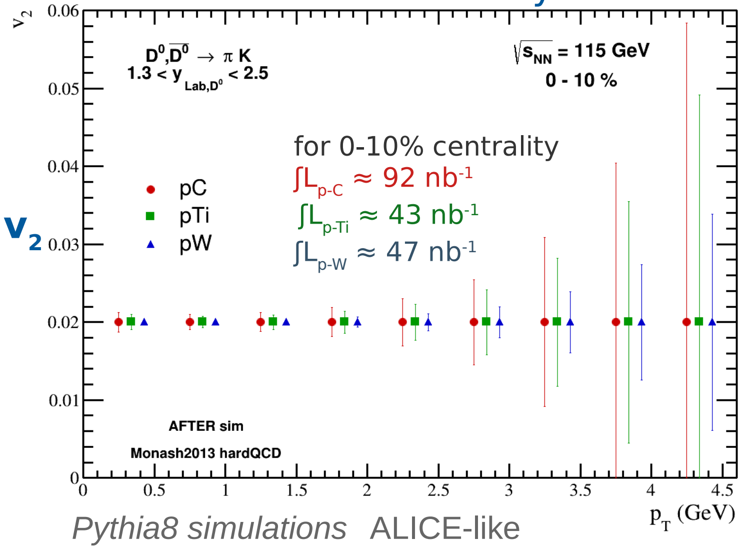

Pythia8 simulations ALICE-like

- ALICE: target at z = -4.7 m, with 1cm long solid targets
- Similar precision expected in 10-20, 20-40% centrality intervals
- Quarkonia and HF μ can be studied with ALICE muon arms at: $-1.6 < y_{CMS} < -0.5$

Quarkonium R_{AA}

- Precise measurements of charmonium states vs rapidity
- Measurement of the 3 Υ(nS) state suppression

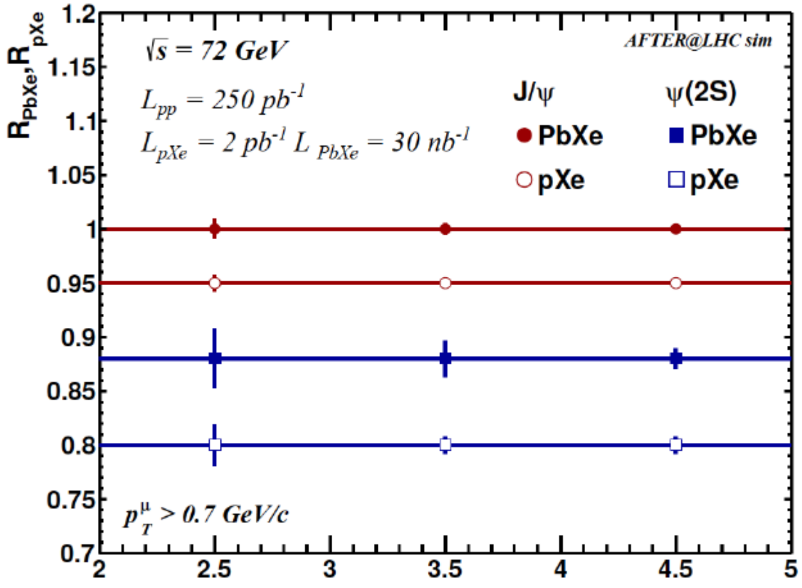

HELAC-Onia+Pythia8 simulations LHCb-like

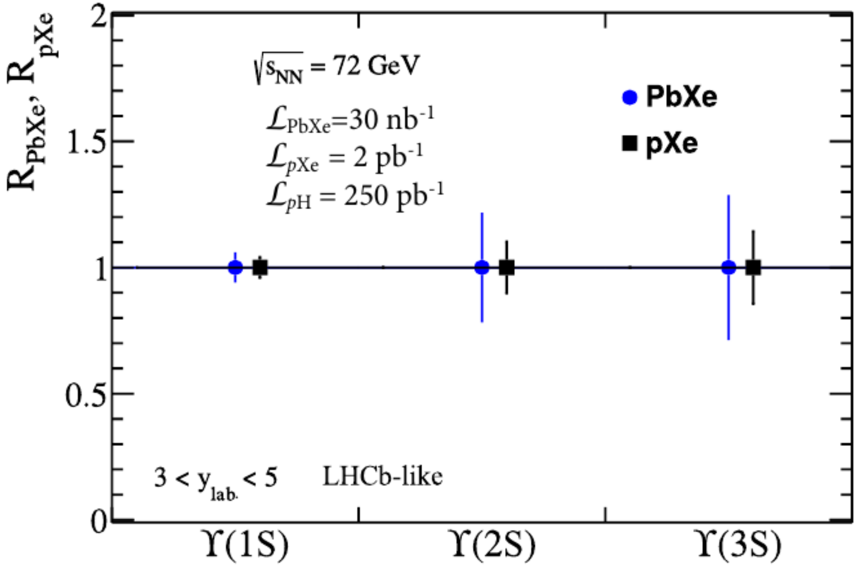

HELAC-Onia+Pythia8 simulations LHCb-like

- Possibility to access χ_C and η_C, J/ψ – J/ψ and J/ψ – D correlations

Few Body Syst. 58 (2017) 5, 148
arXiv: 1807.00603

Decorrelation predictions FT

- ➔ Event-by-event viscous hydrodynamic model
- ➔ Pb-W, Pb-Ti, Pb-C at 72 GeV

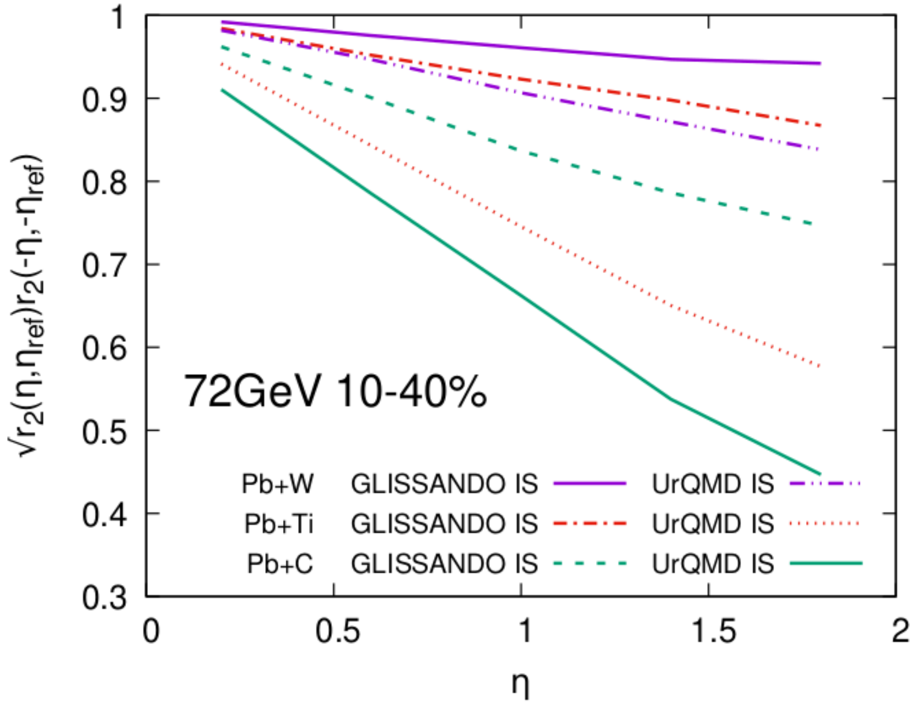

- ➔ **r_n definition**
  - Asymmetric system
    (CMS, Phys. Rev. C92 (3) (2015) 034911):

$$\sqrt{\frac{\langle q_n(-\eta)q_n^*(\eta_{\mathrm{ref}})\rangle}{\langle q_n(\eta)q_n^*(\eta_{\mathrm{ref}})\rangle}\frac{\langle q_n(\eta)q_n^*(-\eta_{\mathrm{ref}})\rangle}{\langle q_n(-\eta)q_n^*(-\eta_{\mathrm{ref}})\rangle}}.$$

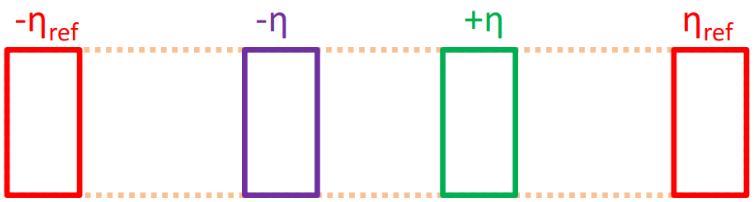

- ➔ Strong decorrelation, increasing with decreasing system size
- ➔ Significant differences between different IS models

STAR r_2 vs models

➔ **STAR r_2 vs models**

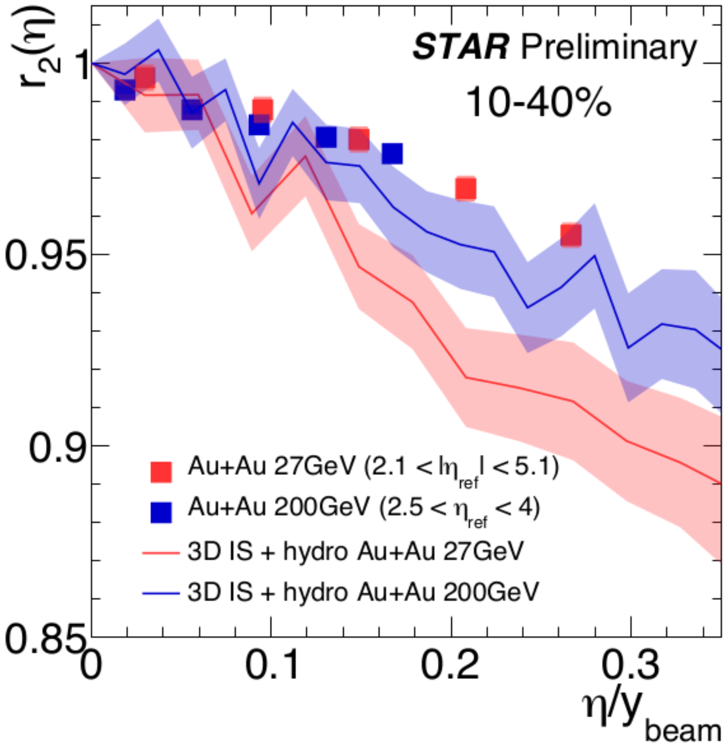

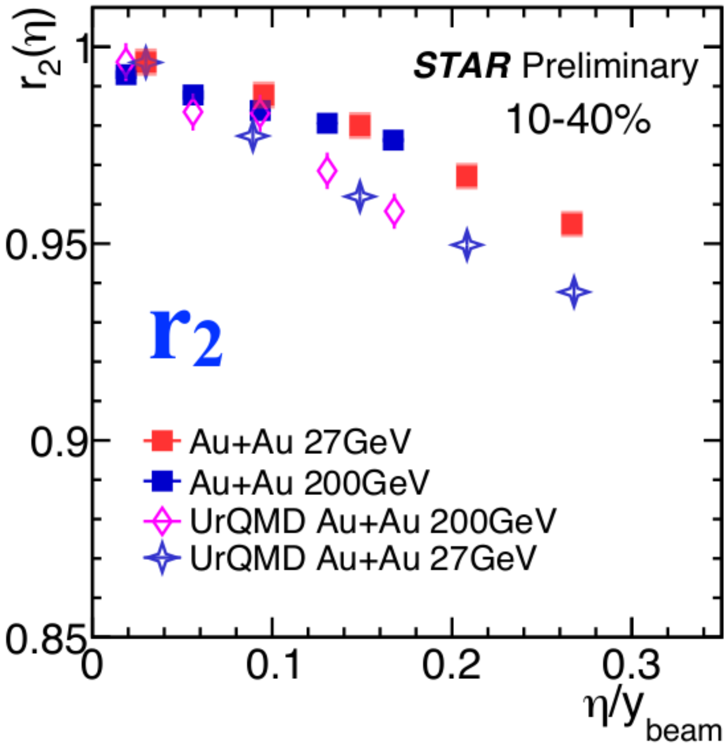

M.Nie, QM19

Local hyperon polarization

- Anisotropic flow → Longitudinal polarization P_z (thermal vorticity + shear term)

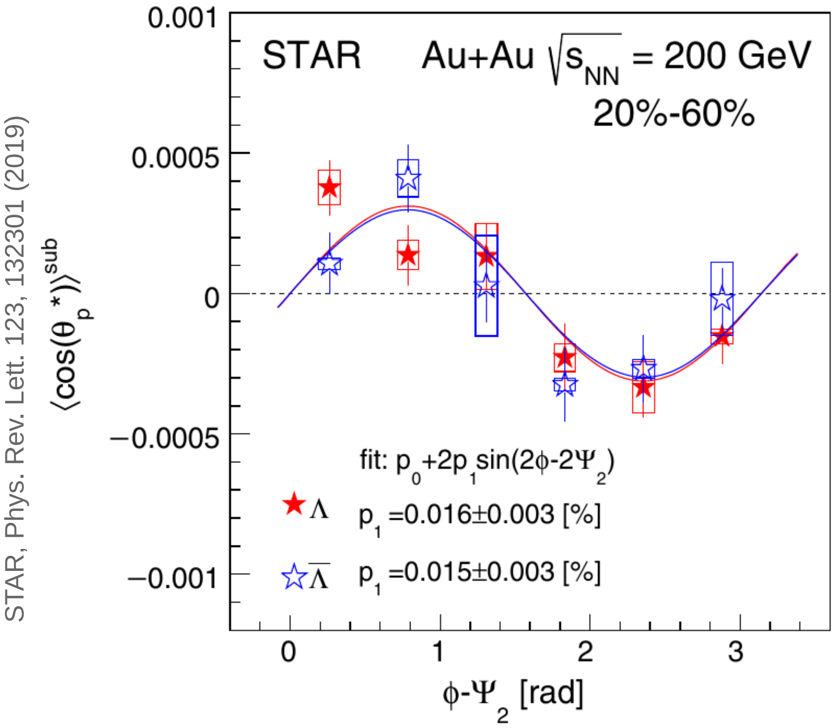

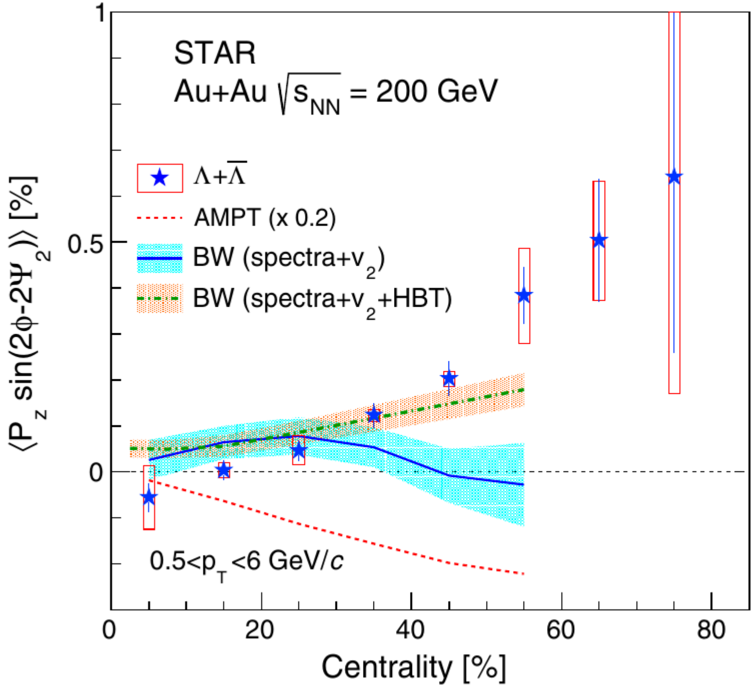

$$P_z = \frac{\langle \cos\theta_p^* \rangle}{\alpha_H \langle \cos^2\theta_p^* \rangle}.$$

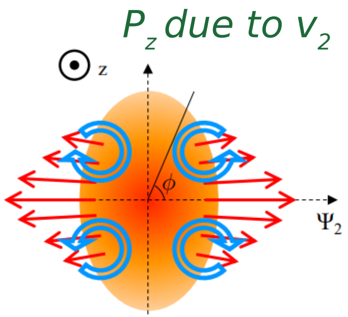

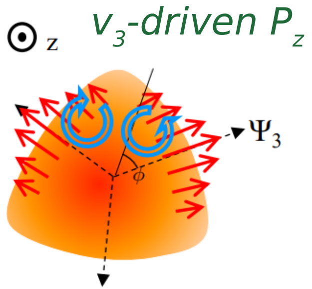

➔ 2^{nd} P_z increase with centrality: additional constraint on shear viscosity

Physics case: QGP (3)

- Study of the **quark-gluon plasma** between SPS and top RHIC energies of $\sqrt{s_{NN}}$ = 72 GeV over broad rapidity range
- Complete studies as a function of rapidity, centrality and system size → **scan in μ_B**
- Explore the longitudinal expansion of the QGP
  - Particle yields and v_n → temperature dependence of the shear viscosity
- Unique access to hard probes at this energy domain
  - Quarkonium suppression in QGP → thermodynamic properties of the QGP
  - D meson R_{AA} and v_2 → heavy-flavour energy loss, transport properties of the QGP
- p-A, lighter ions and high-multiplicity pp collisions
  - Test of collectivity in small systems
  - factorization of CNM effects
    from pA to AB → Drell-Yan
    (insensitive to QGP formation)